PALAIOS
Emphasizing the impact of life on Earth's history

PALAIOS, 2008, v. 23, p. 648–666
Research Article
DOI: 10.2110/palo.2008.p08-033r

ANALYZING VARIATIONS IN CEPHALOPOD ABUNDANCES IN SHELL CONCENTRATIONS: THE COMBINED EFFECTS OF PRODUCTION AND DENSITY-DEPENDENT CEMENTATION RATES

ADAM TOMAŠOVÝCH[1,2]* and JÁN SCHLÖGL[3]

[1]*University of Chicago, Department of Geophysical Sciences, Chicago, Illinois 60637, USA;* [2]*Slovak Academy of Sciences, Geological Institute, Dúbravská cesta 9, 84005 Bratislava, Slovakia;* [3]*Comenius University, Department of Geology and Paleontology, Mlynská dolina G, 84215 Bratislava, Slovakia*
e-mail: tomasovych@uchicago.edu

ABSTRACT

Upper Jurassic ammonoid shell concentrations on pelagic carbonate platforms formed by the mixture of well-preserved and moldic shells provide a unique opportunity to evaluate the effects of average shell durability and productivity on variations in shell abundance preserved in the fossil record. High abundance of primary cement has significantly negative statistical effects on taphonomic alteration, reducing the proportion of ammonoid shells affected by Fe-staining and syndepositional dissolution. High proportions of internal borings indicate that shell concentrations were not rapidly buried. Significantly negative effects of taphonomic alteration on ammonoid shell-packing density and spatial variations in shell-bed thickness show that variations in ammonoid abundance are related to variations in production and destruction rates rather than to variations in sediment dilution. The close spatial association of dissolved aragonite shells and precipitated calcite in shell-rich deposits and the higher proportion of dissolved molds in shell-poor beds demonstrate the simultaneous action of dissolution and cementation in the semiconsolidated mixed layer. These relationships imply positive feedback between the high abundance of ammonoid shells and the low rate of shell destruction, with dissolved carbonate ions from high aragonite input reducing the rate of ammonoid dissolution and providing a local source for carbonate cement. Cementation has the strongest positive relationship with shell-packing density in rank correlations and generalized linear models. Proportions of ammonoid embryonic stages and early juveniles have smaller but significantly positive statistical effects on shell-packing density in simple regressions. We hypothesize that (1) ammonoid shell concentrations correspond to long-term peaks in ammonoid production, with aragonite dissolution buffering the porewater chemistry, and (2) the increase in ammonoid production rates was related to intervals with average high fecundity coupled with high juvenile mortality.

INTRODUCTION

Variations in abundances of fossil organisms have high importance in paleoecological studies because they can be related to variations in proportional or rank abundances, maximum carrying capacity, biomass, or shell-production rate (Kidwell and Brenchley, 1994; Martin, 1996; Brett, 1998; Wignall and Benton, 1999; Payne and Finnegan, 2006). These variations can correlate with or control extinction risk, geographic range, energy flow, or intensity of biotic interactions. Analytical methods that decouple confounding effects of variation in net sedimentation rates and shell-destruction rates from biological variation in population abundances in fossil assemblages, however, are poorly explored (e.g., Kranz, 1977; Powell, 1992; Olszewski, 2004). For example, the relationship between taphonomic alteration and shell abundance that is positive or negative can resolve effects of net sedimentation rates from effects of varying shell destruction and production rates (Kidwell, 1986; Tomašových et al., 2006). Analyses of shell abundance can also be constrained to environments with comparable sedimentation rates (e.g., Payne et al., 2006) and comparable alteration levels and time averaging (e.g., Dattilo, 1996; Peters, 2004; Finnegan and Droser, 2005; Holland and Patzkowsky, 2007) and need to take into account the effects of postmortem transport (e.g., Miller and Cummins, 1990; Zuschin et al., 2005; Tomašových, 2006; Finnegan and Droser, 2008). Distinguishing whether variations in shell abundance are caused by differential diagenesis or by differential productivity can be especially difficult in carbonate successions affected by cementation and redistribution of calcium carbonate (Westphal, 2006). Separation of carbonate production effects from dissolution effects in the preservation of calcareous plankton is also decisive in evaluating temporal changes in seawater chemistry (e.g., Gerhardt and Henrich, 2001; Klöcker et al., 2006).

In this study we use generalized linear models and rank correlations to evaluate influences of sedimentation, shell-production, and shell-destruction rates on variations in shell abundance of cephalopods, specifically the ammonoids. In the fossil record, variations in production rates can be partly approximated by size-specific mortality patterns estimated independently of variations in shell abundance. Ammonoids possessed embryonic calcified shells 1–2 mm in size and, thus, can be used to estimate egg productivity (fecundity) or embryonic mortality generally not available owing to the low-preservation potential of eggs. Juvenile mortality can be approximated by variations in size-frequency distributions, assuming size-frequency distributions are stable or stationary through the period of time averaging. Ammonoids thus provide the unique opportunity to estimate variations in abundances of embryos and juvenile mortality of ammonoid populations averaged over the interval of sediment deposition, which can be compared with variations in the shell abundance of adults. This is in contrast to such benthic shell-bed producers as brachiopods and bivalves that have minimal preservation potential of embryonic stages. Although growth and dispersal rates remain poorly constrained for ammonoids, evaluation of the statistical effects of durability and productivity indicators on shell abundance provides insights into ammonoid population dynamics, explains the formation of ammonoid shell concentrations, reveals the source of aragonite for carbonate cement, and has implications for taphofacies analyses.

Ammonoid shell concentrations used in this study originated in widespread environments of pelagic carbonate platforms in the western part of the Tethys Ocean during the Late Jurassic–earliest Cretaceous (Kimmeridgian–Berriasian). Pelagic carbonate platforms were fault-bounded submarine highs characterized by extremely reduced carbonate sedimentation rates and situated at great distances from terrigenous input (Santantonio, 1994). Sediment starvation, bioturbation, and dissolution-cementation processes dominated these settings and are comparable to those of present-day seamounts (Garrison and Fischer, 1969; Jenkyns, 1971; Santantonio, 1994; Clari and Martire, 1996). Such conditions were widespread also during other time intervals (Wendt et al., 1984). Sediment-starved carbonates of pelagic platforms are commonly marked by red staining (van der Kooij et al., 2007) and are characterized by the

* Corresponding author.

 0883-1351/08/0023-0648/$3.00

frequent occurrence of shell concentrations (Kutek and Wierzbowski, 1979; Cecca, 1992; Conti and Monari, 1992; Krobicki, 1994; Olóriz et al., 1996).

Three hypotheses can explain variations in abundance of ammonoids shells on pelagic carbonate platforms. First, condensed successions are beneficial for preservation of shell concentrations owing to the lack of sediment (sediment-dilution hypothesis). The reduced-sedimentation rate is assumed to be one of the major causes of the presence of ammonoid shell concentrations on pelagic carbonate platforms (Wendt, 1973; Martire, 1992, Santantonio, 1993) and in other carbonate environments (Gómez and Fernández-López, 1994). The presence of concentrations with originally aragonitic shell producers within condensed successions is enigmatic because nodular limestones, bioclastic limestones, and hardgrounds on pelagic carbonate platforms show signs of substantial dissolution of aragonite shells (Olóriz et al., 1996; Preto et al., 2005). Such environments were affected by high shell-destruction rates deleterious for formation of shell concentrations with aragonite producers. Second, under high input of aragonite due to high input of platform-derived aragonitic mud or high ammonoid-production rates, syndepositional aragonite dissolution can be an important source for neomorphic replacement and precipitation of calcite cement that enhances durability of shells against destruction (Hendry, 1993; Palmer and Wilson, 2004). This buffering effect of aragonite dissolution and subsequent cementation therefore may partly explain this apparent paradox (differential-cementation hypothesis). Third, fluctuations in the biomass-production rate owing to changes in fecundity, growth, and mortality lead to changes in density of ammonoid populations that can be captured by variations in shell abundance in fossil assemblages (differential-productivity hypothesis). In contrast to *Nautilus*, ammonoids had small embryos <2 mm in diameter, little parental investment per egg based on large adult-size to embryo-size ratio, and produced a large number of offspring with high juvenile mortality based on dense concentrations of ammonitellas—shells that extend up to the primary constriction and varix—and high abundance of juveniles relative to adults (Landman et al., 1983; Manger et al., 1999). Preservation of ammonoids in shell concentrations thus can be enhanced by their propensity to form populations with high standing biomass and characterized by high population-turnover rates. This is based on the assumption that ammonoids possessed a reproductive and life-history strategy similar to that of some present-day coleoids (Bucher et al., 1996, Landman et al., 1996). Modern coleoid species are characterized by exceptionally high standing-population density, rapid population turnover, and high growth efficiency and are commonly characterized by high post-spawning mortality (Boyle and Boletzky, 1996; Clarke, 1996; Wells and Clarke, 1996; Boyle and Rodhouse, 2005).

Although highly abundant ammonitellas and juvenile ammonoids are found widely in late Paleozoic and Mesozoic deposits (Kulicki and Wierzbowski, 1983; Ward and Bandel, 1987; Tanabe et al., 1993, 1995), they do not provide conclusive evidence for higher-than-average fecundity or higher-than-average embryonic and juvenile ammonoid mortality. In addition to population dynamics, their abundance in strata is also driven by the interplay of nonbiological factors related to sedimentation and shell-destruction rates (Kidwell, 1986, 1991; Maeda and Seilacher, 1996; Floquet et al., 2003; Reboulet et al., 2003). Note that these concentrations with early ontogenetic stages were reported from time intervals characterized by calcite-dominated as well as by aragonite-dominated seawater chemistry (e.g., Sandberg, 2003; Hardie, 1996; Riding and Liang, 2005).

Three specific goals of this study are aimed at quantifying the effects of sedimentation, shell production, and shell destruction on the origin of ammonoid shell concentrations. First, univariate and multivariate analyses are used to evaluate ammonoid taphofacies and taphonomic pathways that lead to preservation of ammonoids. Second, shell-packing density of ammonoids is related to proportions of dissolved ammonoid shells and carbonate cement. Third, the relationship between ammonoid shell-packing density (excluding ammonitellas and early juveniles), the proportion of embryonic stages (ammonitellas), and the proportion of early juvenile ammonoids are assessed to evaluate the statistical effects of embryo abundance and juvenile mortality on the shell-packing density of larger ammonoids. This approach is analogous to analyses that model relationships between fecundity, mortality, and population density in benthic invertebrates (Stillman et al., 2000; Van der Meer et al., 2001; Beukema and Dekker, 2007).

EFFECTS OF MORTALITY ON SHELL ABUNDANCE: A MODEL

Population density of closed populations increases by increased fecundity, decreased mortality of individual age classes, or by their combination. Modern coleoid populations are controlled by variations in (1) fecundity due to spawning success (Coelho et al., 1994), (2) embryonic mortality from temperature and salinity fluctuations (Steer et al., 2002), or (3) postembryonic juvenile mortality from susceptibility of juveniles to environmental variability and low zooplankton productivity (Waluda et al., 1999). Relationships between population density and vital rates can be complex and depend on covariation and on the magnitude of fecundity and mortality. The sign of the relationship between population density and juvenile mortality can be diagnostic for different life histories regulated either by variations in fecundity or by variations in juvenile mortality. Expected qualitative relationships between population density on the one hand and fecundity and mortality on the other hand are shown in three scenarios with (1) random fluctuations of fecundity and juvenile mortality with uncorrelated demographic and environmental stochasticity, (2) negative covariation between fecundity and juvenile mortality, and (3) positive covariation between fecundity and juvenile mortality. We explore temporal variations in population dynamics of single species with a density-dependent model and discrete generations with the equation

$$N_{t+1} = \frac{b(1 - d)N_t}{1 - \alpha N_t}$$

where N_{t+1} is the density of individuals of species in time step $t + 1$, b is the density-independent fecundity (the number of eggs), d is the density-independent mortality rate of juveniles (the probability that an individual dies from the time of its hatching to maturity or adulthood), and α is the intraspecific competition coefficient (e.g., Watkinson, 1980; Watkinson et al., 2003). To model demographic stochasticity, fecundity values follow a Poisson distribution, and the number of surviving juveniles follows a binomial distribution (e.g., Akçakaya, 1991; Adler et al., 2007). To model uncorrelated environmental stochasticity in the simulation with random fluctuations of vital rates, fecundity and survivorship—the number of surviving juveniles—are multiplied by a number randomly drawn from the uniform distribution in the interval from zero to one (Fig. 1A). We use a sine function to model nonrandom autocorrelated environmental variations with the fixed length of wave period in the simulations with positive and negative covariations of fecundity and juvenile mortality (Figs. 1B–D). In these scenarios with discrete generations, population turnover corresponds to one time step, and the expected production rate (i.e., expected shell abundance in death assemblages) is thus proportional to abundance of adults in living populations.

Under random and unpredictable fluctuations of vital rates with white-noise dynamics (i.e., rates are not temporally correlated; see Akçakaya et al., 2003), fecundity is positively and juvenile mortality is negatively related to population density (Fig. 1A). The shapes of these relationships are triangular in bivariate plots, however, because fecundity and mortality have confounding effects on each other (Fig. 1A). Under negative covariation between fecundity and juvenile mortality, the production rate is increased by high investment in reproductive effort and by low juvenile mortality. In this case, fecundity increases and juvenile mortality decreases with increasing population density (Fig. 1B). Under positive covariation between fecundity and juvenile mortality, the shape of the relationship between population density and vital rates depends on the magnitude of

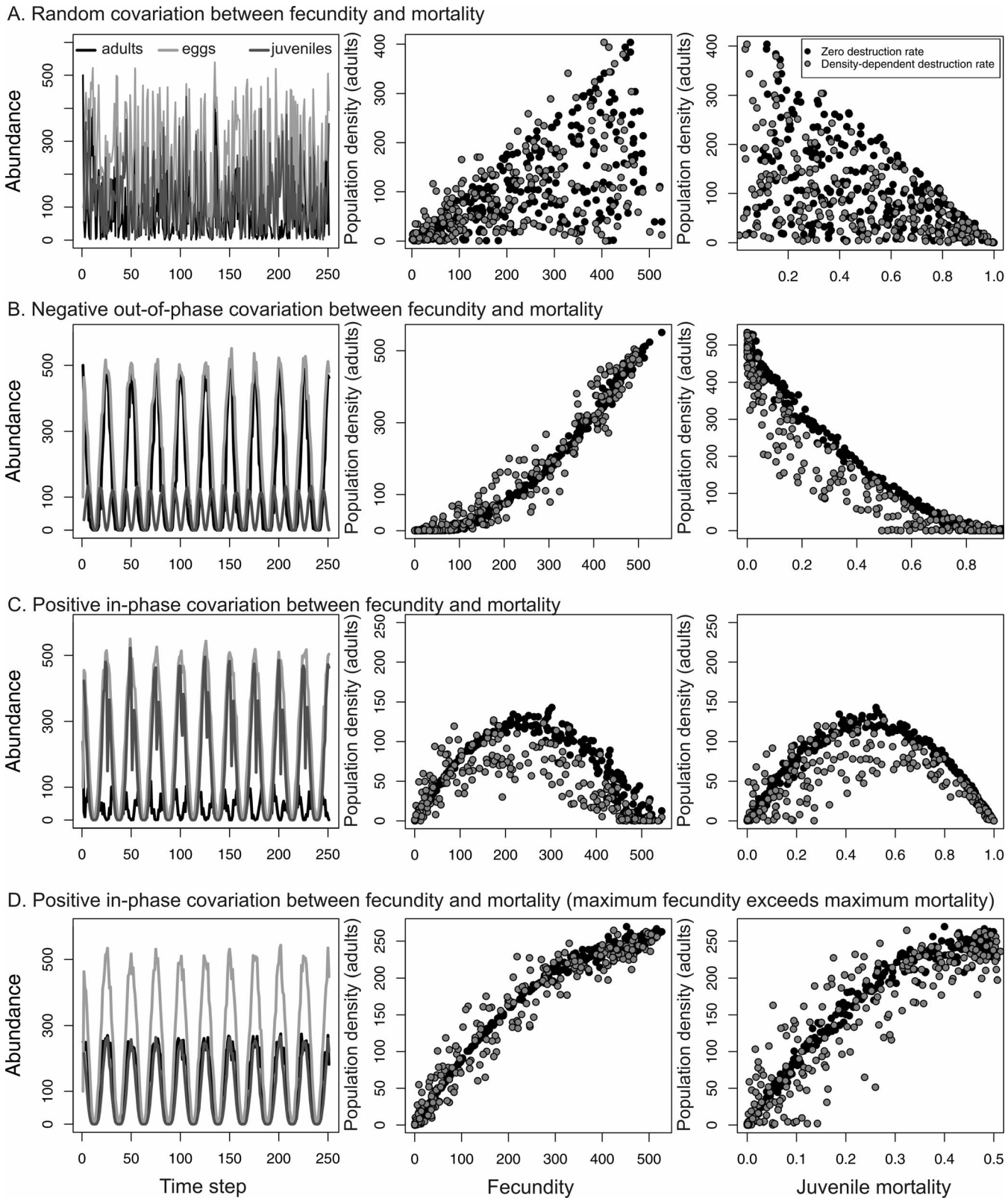

FIGURE 1—Four scenarios showing temporal changes in the abundance of adults, eggs, and early juveniles (plots on the left) and predicting the sign of the relationships between population density (number of adults) and fecundity (number of eggs, middle plots) and between population density and juvenile mortality (proportion of juveniles, plots on the right) under no taphonomic loss (black points) and density-dependent destruction rates (gray points). They predict that the relationship between juvenile mortality and population density is negative but can be positive for the positive covariation model (D). A) Random covariation between fecundity and mortality. B) Negative out-of-phase covariation between fecundity and mortality. C) Positive in-phase covariation between fecundity and mortality. D) Positive in-phase covariation between fecundity and mortality (maximum fecundity exceeds maximum mortality). For illustrative purposes, parameter values are fecundity = 500 eggs; sine wave period in B–D = 25 time steps.

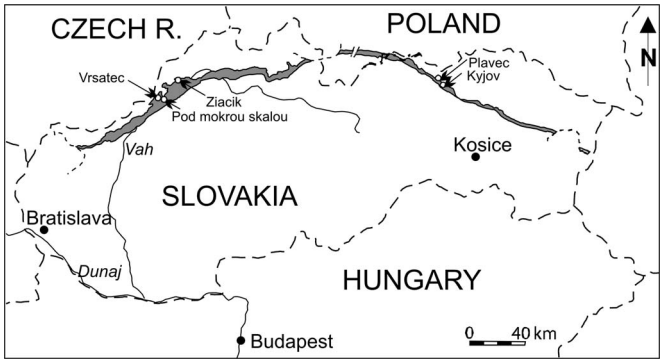

FIGURE 2—Location of five localities with pelagic carbonate platform deposits of the Czorsztyn Ridge in the Pieniny Klippen Belt (gray shaded area) in the West Carpathians.

fecundity and mortality. When fecundity and mortality have equal magnitudes and perfectly covary in phase, population density initially increases and then decreases with increasing fecundity and mortality (Fig. 1C). When fecundity is substantially higher than mortality, population density covaries positively with mortality. In Figure 1D, fecundity exceeds mortality by a factor of two, and the maximum mortality rate is thus 0.5. The highest population density corresponds to the highest fecundity and the highest juvenile mortality. This mode leads to a high production rate via high fecundity (but not low mortality). The positive relationship between juvenile mortality on one hand and shell abundance on the other hand, therefore, can distinguish the scenario in which increase in fecundity primarily contributes to high population density from other scenarios in which reduced juvenile mortality is also enhancing population density. We note that variations in abundances of ammonitellas in fossil assemblages are affected both by fecundity and embryonic mortality, but the sign of the relationship between abundance of ammonitellas and shell abundance of adults also reveals whether adult shell abundance is linked to combined effects of fecundity and embryonic mortality.

To approximate taphonomic pathways in the ammonoid shell concentrations, we model shell destruction as a stochastic rate with linear negative dependence on shell abundance in death assemblage. This negative density-dependence ensures that relationships between population density and vital rates are preserved in fossil assemblages. Time averaging is generally expected to decrease temporal variations in abundances due to the decrease in temporal resolution (Kowalewski, 1996; Olszewski, 1999). It therefore should not reverse the general sign of the relationship between population density and mortality patterns—this effect is analogous to the decrease in spatial variability in species abundances with decreasing spatial resolution.

METHODS

Sections

Ammonoid deposits from the Upper Jurassic to the lowermost Cretaceous (Kimmeridgian–Berriasian) Dursztyn Formation at five localities of the Pieniny Klippen Belt (West Carpathians) were analyzed: Vršatec, Žiačik, Pod Mokrou Skalou, Kyjov, and Plaveč (Fig. 2). These localities form an ~200-km-long, E–W oriented transect along the so-called Czorsztyn Ridge that preserves deposits formed on a pelagic carbonate platform in the Western Tethys (Birkenmajer, 1986). Small-scale spatial variations in ammonoid preservation were evaluated in two closely positioned sections at Vršatec and Kyjov. The Dursztyn Formation is only ~10–25 m thick and likely reflects very low sedimentation accumulation in environments below the photic zone because light-dependent benthic organisms are invariably rare or absent.

Analyses of Ammonoid Preservation

The taphonomic alteration of ammonoids was determined by thin-section analysis, at the level of the subclass Ammonoidea. Although members of the Phylloceratina, Lytoceratina, and Haploceratidae dominate the ammonoid assemblages of the Dursztyn Formation, their identification is not possible in thin section. This analysis is thus conservative in finding nonrandom relationships between mortality patterns and shell abundance because life history strategies can differ among ammonoid species.

We scored the presence or absence of six variables in all ammonoid shells and fragments >1 mm in thin section under the binocular microscope at 25× magnification: fragmentation, bioerosion, Fe-stained coating, Fe-stained boring infill, encrustation, and syndepositional dissolution of shells and fragments (see Supplementary Data[1]). Encrustation refers to the presence of sessile foraminifers and serpulids attached to ammonoids (Fig. 3A). Bioerosion refers to the presence of microborings in neomorphosed or moldic shells and fragments (Figs. 3B–C). Fe-stained coating and Fe-stained infill correspond to thin microbial crusts and boring infill impregnated by Fe-minerals, respectively (Figs. 3C–D). Crusts locally consist of wavy-laminated, nonfenestrate layers, the microproblematicum *Frutexites*, and oncoids (Böhm and Brachert, 1993).

Syndepositional dissolution refers to ammonoid molds affected by wholesale syndepositional dissolution and subsequent void-filling cement precipitation or infiltration by interstitial micrite, indicating infiltration of soft sediment (e.g., Sanders, 2003). Such ammonoids are represented by (1) completely dissolved remnants represented by molds filled with interstitial micrite and coated by Fe-crusts or encrusters (Figs. 3C–D), (2) molds filled with interstitial micrite or microspar, with thin relict shell walls preserved as neomorphic calcite (Fig. 3E), or (3) molds with completely dissolved shell layers and differential sediment infill relative to the neighboring sediment (Fig. 3F). Well-preserved neomorphosed ammonoid shells with relicts of fine-scale shell structure are calcitized—that is, ultimately affected by aragonite dissolution and calcite replacement (Tucker and Wright, 1990). Shells with this type of preservation, however, do not show signs of multiple exhumation and burial, and their calcification likely took place during final burial.

The proportion of altered shells and fragments was computed relative to the total number of shells and fragments. Shells and fragments that show bioerosion, Fe-stained coating, Fe-stained infill, and encrustation on both sides of ammonoid remnants are scored as altered. The sample size in 44 thin sections ranged between 17 and 134 ammonoid fragments and shells (median = 58). Maximum dimensions of all specimens were measured in thin-section.

We estimated statistical effects of (1) the proportion of primary porosity cement (microspar and spar) filling voids in shells and cavities, (2) the proportion of micrite, and (3) the proportion of shells >5 mm (relative to the total number of individuals) on ammonoid preservation. We note that statistical effects are not equal to causal effects. Proportions of cement and micrite were estimated using percentage-estimate comparison charts and 5% intervals (Bacelle and Bosellini, 1965). The primary cement is represented by scalenohedral cement, epitaxial calcitic overgrowths, and radiaxial calcite that originated as void-filling cement (Kendall, 1985) or as replacement of primary magnesian calcite cement (Wilson and Dickson, 1996). The proportion of shells >5 mm relative to the total number of individuals is based on measurements of maximum dimensions of individual ammonoids in thin section.

Nonmetric multidimensional scaling (NMDS) is a multivariate analysis tool that we used to evaluate similarities in ammonoid preservation among samples with the Manhattan distance. Analysis of similarities (ANOSIM) is a categorical, distance-based test (Clarke and Green, 1988) that we used to evaluate differences in taphonomic alteration among three ammonoid deposit types, including (1) floatstones, (2) rudstones, and (3) packstones-grainstones, and spatial differences in preservation among

[1] www.paleo.ku.edu/palaios

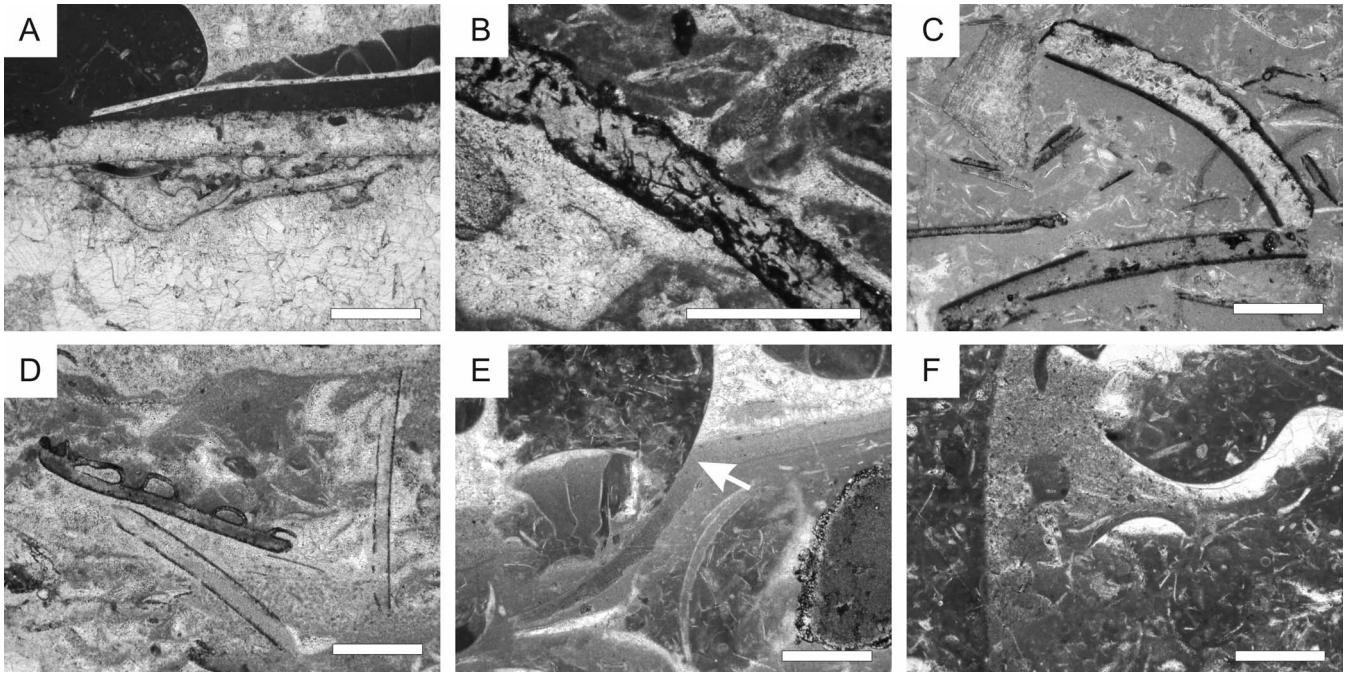

FIGURE 3—Preservation of ammonoids in thin section. Scale bars = 1 mm. A) Sessile foraminifers encrusting the internal side of a neomorphic shell wall; Kyjov II bed 20. B) Strongly bored recrystallized shell fragment with Fe-stained microborings; Žiačik bed 4. C) Dissolved shell fragments filled with internal micrite and coated with Fe-stained crusts; Žiačik bed 13. D) Fe-stained and dissolved fragments filled with micrite in continuity with neighboring matrix; Žiačik bed 4. E) Close association of syndepositional dissolution (arrow) and precipitation of radiaxial cement. Note, dissolved fragments were not coated; Kyjov I bed 21. F) Partly dissolved ghost of ammonoid shell distinguishable by a lighter micrite infill relative to the neighboring dark micrite (arrow); Plaveč bed 16.

three localities with more than three samples (Vršatec 2, Žiačik, and Kyjov). In addition, we used ANOSIM to evaluate whether there are any differences in size-frequency distributions of ammonoid remnants among the three ammonoid deposit types.

We used univariate analysis to evaluate statistical effects of three factors—cement, micrite, and shells >5 mm—on taphonomic alteration with generalized linear models (GLM). The response variables are (1) the overall assemblage-level alteration represented by sample scores along the first NMDS axis and (2) proportions of six taphonomic variables. We used the logit-link function and the quasi-binomial variance function because response variables are proportions that vary between zero and one, residuals do not follow normal distribution, and quasi-binomial models estimate the dispersion parameter directly from the data. Our analyses are affected by multicollinearity (intercorrelation) among proportions of cement, micrite, and shells >5 mm. Multicollinearity can increase standard errors of regression coefficients and, thus, makes our findings of regression-slope significance conservative. We also assessed the statistical effects of cement, micrite, and shell size on six taphonomic variables with canonical analysis of principal coordinates (CAP; Anderson and Willis, 2003; Oksanen et al., 2005). This method allows the use of such non-Euclidean dissimilarity indices as Manhattan distance. First, it ordinates the distance matrix with principal coordinate analysis, then it performs unweighted linear regression of three factors on principal coordinate axes. Canonical analysis of principal coordinates does not display all variation in the data, only that part that is significantly explained by three constraining factors.

Analyses of Effects of Alteration on Shell Abundance

Shell abundance was measured as shell-packing density that corresponds to the areal proportion of ammonoid shells and fragments >5 mm observed per 20 cm^2—excluding embryonic stages and early juveniles. This is estimated in thin section using percentage-estimate comparison charts and 5% intervals. It is important to note that this measure includes both well-preserved shells as well as moldic shells affected by syndepositional dissolution. The amount of syndepositionally dissolved aragonite can be approximated as the proportion of dissolved (moldic) shells multiplied by shell-packing density. This measure of dissolved aragonite does not take into account shells that were rapidly dissolved in unconsolidated sediment, but it does provide some information about the amount of dissolved aragonite in semilithified zones affected by bioturbation and sediment reworking. In order to distinguish the effects of sedimentation and shell-input (production and destruction) rates on shell-packing density and to evaluate the sign of the correlation between taphonomic alteration and shell-packing density (or shelliness; see Tomašových et al., 2006), GLM was used with shell packing-density as the response variable and the overall taphonomic alteration (first NMDS axis) as the predictor variable.

Analyses of Effects of Durability and Productivity on Shell Abundance

Two indicators of shell durability were used. First, proportions of altered shells can be proportionally related to shell destruction rates, assuming equilibrium and relatively complete time-since-death frequency distribution of ammonoid shells (Tomašových et al., 2006). Second, proportion of cement in intrashell cavities and shelter pores was used as an indicator of shell durability owing to the positive relationship between the saturation state and cement formation. These two variables are highly positively correlated, and results are presented using the proportion of cement only. The presence of primary cement implies pore-water chemistry that decreases shell susceptibility to dissolution. Although the presence of primary cement can be affected by the availability of pore spaces—under high fragmentation, shells can be degraded to small fragments that provide very restricted pore space for cement—our analyses indicate that fragmentation levels are invariably high and relatively constant across samples.

To evaluate abundance of embryonic stages, we counted proportion of ammonitellas per 5 mm^2 in micritic portions of thin sections relative to the number of other microplankton groups. In thin sections of the Dursztyn Formation, ammonitellas are generally <1 mm. Ammonitellas were

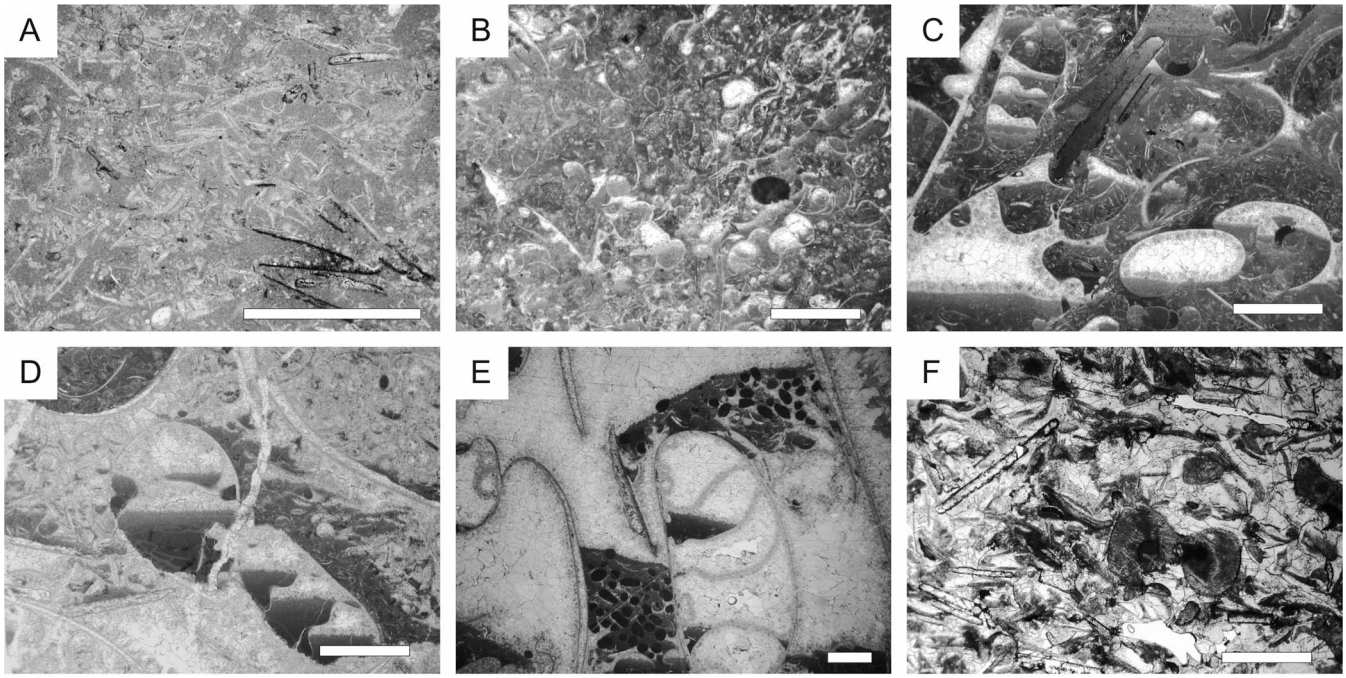

FIGURE 4—Microfacies with deposit types with ammonoids. Scale bars = 2 mm. A) Floatstone with rare ammonitellas and dominated by the planktic crinoid *Saccoccoma*; Žiačik bed 10. B) Floatstone with abundant ammonitellas; Pod Mokrou Skalou bed 3. C) Floatstone with concordantly oriented ammonoids and shelter cement; Kyjov I bed 21. D) Ammonoid rudstone with sparitic shelters, intraskeletal cement, interstitial micrite, and accumulations of ammonitellas; Pod Mokrou Skalou bed 11. E) Ammonoid rudstone with sparitic shelters and intraskeletal cement and accumulations of fecal pellets; Kyjov II bed 20. F) Crinoidal grainstone with poorly preserved and coated ammonoid fragments; Žiačik bed 18.

probably neutrally buoyant after hatching and lived as plankton in the water column (Shigeta, 1993; Landman et al., 1996). The standardization of ammonitella density relative to the number of other similar-sized plankton groups alleviates confounding effects of winnowing and differential sedimentation rates among samples.

Early juvenile postembryonic stages are represented by the neanic stage (neanoconch) with little or no ornamentation (3–5 mm in size) that extends approximately two whorls beyond the ammonitella. We used 5 mm as the approximate upper cutoff for assignment of ammonoids to early juveniles and counted the number of all early juvenile shells in thin sections. We estimated their proportion relative to shells >5 mm, assuming stable or stationary size-frequency distribution over the duration of time averaging, excluding fragments not assigned to these stages. Late juvenile stages of ammonoids include all whorls up to the start of the mature body chamber (Bucher et al., 1996), and thus they cannot be distinguished from individuals with body chambers in thin section.

To evaluate effects of shell durability and productivity indicators on shell-packing density, we used simple and multiple GLM with the logit-link function and the quasi-binomial variance function. Multiple GLM simultaneously evaluates unique statistical effects of durability and productivity on shell-packing density (e.g., variance in shell-packing density explained solely by the predictor variables). It is important to note, however, that GLM can be compromised because indicators of durability and productivity are not fixed and are probably not independent of the response variable (shell-packing density) owing to density-dependent population dynamics and density dependence of shell destruction rates. For example, high density of large-sized ammonoids in single-event shell concentrations can correspond to mortality of adult cephalopods immediately after spawning, and spawning in turn causes high abundance of embryonic stages and early juvenile ammonoids (e.g., Doyle and MacDonald, 1993). Estimates of slope coefficients, thus, can be biased (Quinn and Keough, 2002). We therefore also evaluated (1) relationships between durability, productivity, and shell-packing density with Spearman rank correlations and partial Spearman rank correlations that control for other predictor variables (Kim and Yi, 2007), and (2) compared medians of cement proportions, proportions of ammonitellas, and proportions of early juveniles between shell-poor and shell-rich deposits with the Wilcoxon test. Predictor variables were standardized to Z-scores in all GLM analyses.

RESULTS

Ammonoid Deposit Types

Three general types of deposits—red, poorly sorted, shell-poor floatstone; light-gray, poorly to moderately sorted, shell-rich rudstone; and light-gray, well-sorted packstone and grainstone—are distinguished based on sorting and packing of ammonoids. Floatstones are moderately bioturbated and contain poorly sorted and dispersed to loosely packed ammonoids; median shell packing density is 0.1. Floatstone either forms relatively homogeneous sets of massive and poorly bedded limestones or several centimeter-thick layers that alternate with shell-rich rudstones. Floatstones also show a centimeter-scale complex internal stratification of layers that differ in abundance of microplankton, including ossicles of the planktonic crinoid *Saccoccoma* (Fig. 4A), ammonitellas (Fig. 4B), radiolarians, and calpionellids. Larger ammonoids are randomly or concordantly oriented (Fig. 4C). Benthic crinoids, ammonoid fragments, aptychi, and brachiopod fragments dominate skeletal remains. Intraclasts and exhumed, repeatedly bored, coated, and dissolved bioclasts are locally common. Truncated bioclasts were not observed, although firmgrounds are visible in several samples. Intraskeletal pores and shelters are filled by radiaxial and scalenohedral cement (0.15).

Rudstones are poorly or moderately sorted, densely packed, and dominated by large fragments of ammonoids, aptychi, benthic crinoids, and brachiopod fragments. Median ammonoid shell packing density is 0.25. They either form 1-m-thick limestone beds characterized by internal microstratigraphy or alternate with floatstone, packstone, and grainstone. Rudstones are locally laterally discontinuous. Rudstones with micrite-rich matrix show random orientation of bioclasts. Cement-dominated rudstones show preferred orientation of imbricated, convex up-oriented, or stacked ammonoid shells and fragments (Figs. 4D–E). Infiltrated micrite

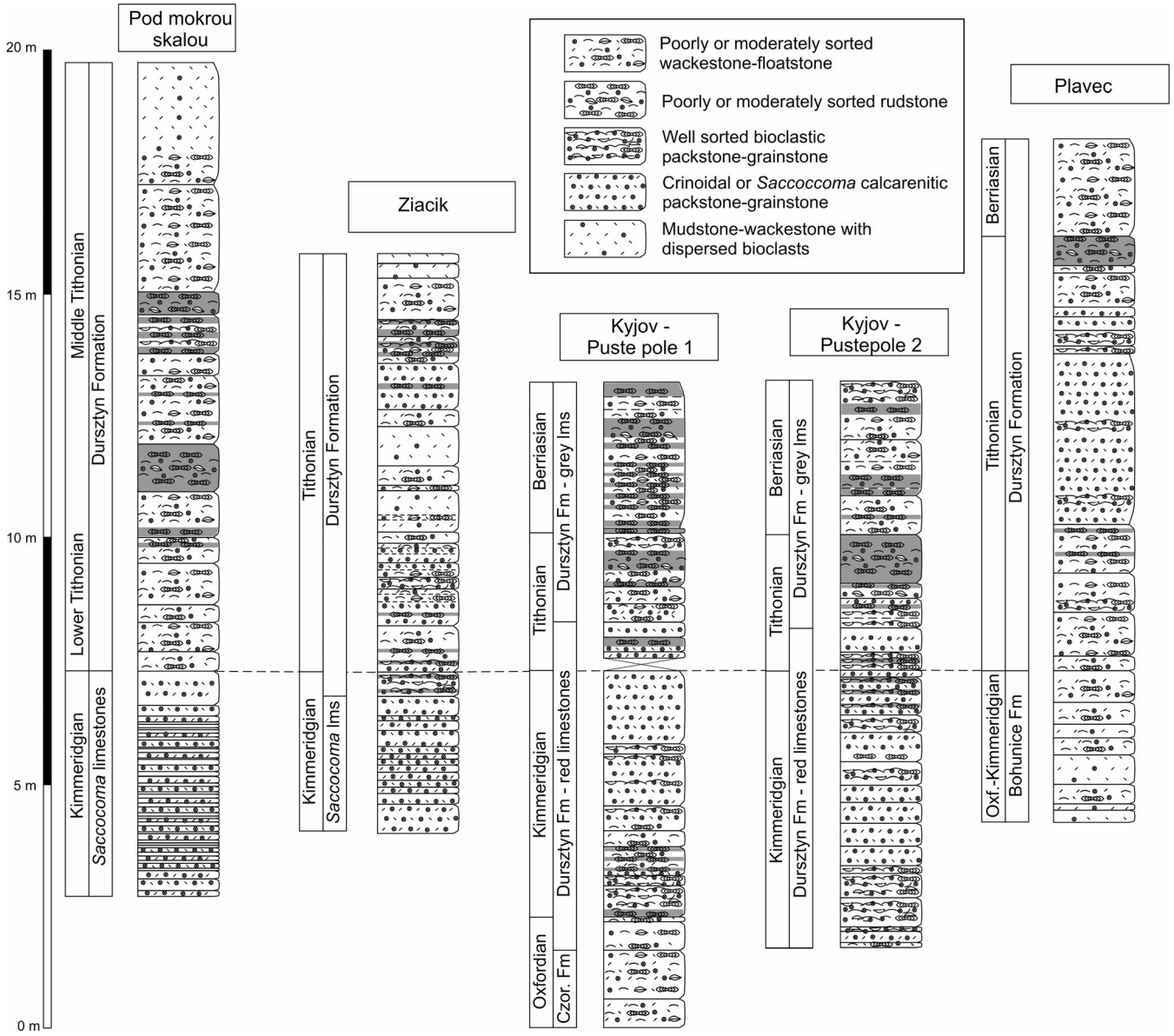

FIGURE 5—Temporal variations in the frequency and thickness of three ammonoid deposit types, showing a decimeter-scale vertical alternation of floatstone, rudstone, and packstone-grainstone in five sections through the Dursztyn Formation along a 200-km-long E–W oriented transect along the Czorsztyn Ridge. Gray-colored beds rich in shelter and intraskeletal cement; these generally correspond to rudstone. Dashed line represents the correlated boundary between the Kimmeridgian and Tithonian.

among shells commonly fills uncemented voids. The base of rudstones is abrupt in terms of a rapid vertical change in shell-packing density, surfaces show centimeter-to-millimeter-scale irregularities, and some layers are graded and show signs of small-scale cross-stratification.

Packstone and grainstone are well sorted (2 mm), densely packed, and locally internally stratified into thin packstone and grainstone layers that differ in packing, sorting, and cement proportion. The rock types either alternate with rudstones or form thick sheets of uniform calcarenites. They are dominated by fragments of benthic crinoids and *Saccoccoma* with epitaxial overgrowths (Fig. 4F). Median ammonoid shell-packing density is 0.1.

Temporal and Spatial Variation in Ammonoid Deposits

In the western parts of the Pieniny Klippen Belt, the Kimmeridgian deposits are represented by uniform sets of packstone and grainstone dominated by the crinoid *Saccoccoma*. In the eastern part, the Kimmeridgian part of the Kyjov section consists of bioclastic packstone-grainstone that alternates with floatstone and rudstone with common ammonoids. The Kimmeridgian deposits of the Plaveč section are represented by uniform sets of floatstone. The lower–middle Tithonian portions of the Dursztyn Formation are characterized by centimeter-scale to decimeter-scale complex stratification formed by alternation of floatstone, rudstone, and grainstone-packstone (Fig. 5). This stratification is preserved in ~10-m-thick successions of lower–middle Tithonian deposits in the Žiačik and Mokrá Skala sections, as well as in the Tithonian and Berriasian deposits of the Kyjov and Plaveč sections.

At small spatial scales, rudstone forms spatially limited layers or lenses that change in thickness across several meters in the Kyjov sections in the eastern parts of the Pieniny Klippen Belt. Fine-scale variation in the fabric of deposit types is pronounced along the distance of several hundreds of meters in the Vršatec sections in the western parts of the Pieniny Klippen Belt (Fig. 6). In the Vršatec 1 section, the Kimmeridgian–lower

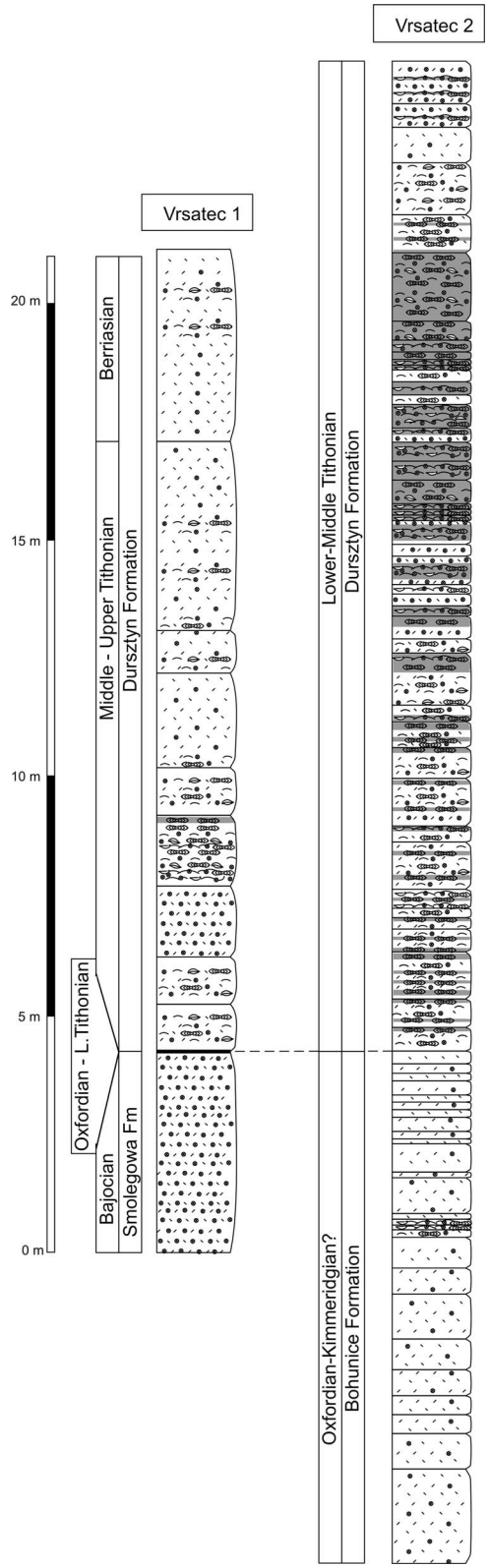

FIGURE 6—Spatial variations in the frequency of three ammonoid deposit types across a distance of about 500 m in the Vršatec sections; decrease in the frequency of shell concentrations corresponds to the decrease in sediment thickness. Lower Tithonian deposits represented by a hardground in the eastern section (Vršatec 1) and by an ~25-m-thick set of ammonoid floatstone and rudstone in the western section (Vršatec 2).

Tithonian deposits up to the *Hybonoticeras hybonotum* Zone are condensed within a several centimeters-thick interval capped by a hardground, and the remaining part of the middle–upper Tithonian is represented by an ~12-m-thick succession of floatstone with occasional rudstone (Vršatec 1, Fig. 6). In contrast, ammonoid shell concentrations in the Vršatec 2 section are found in an ~20-m-thick succession of thick-bedded rudstone alternating with packstone and floatstone that record the lower–middle Tithonian (Vršatec 2, Fig. 6). A relatively thick succession with shell concentrations is, therefore, reduced to a very thin succession with shell-poor deposits across the distance of about 500 m. This spatial replacement shows that shell concentrations do not converge toward areas with condensed sediment thickness and that some areas were characterized by a total lack of deposition for long periods of time; signs of erosional truncation are rare.

At large spatial scales, there are also significant differences in ammonoid preservation among two localities (Vršatec and Žiačik) in the western parts and one locality (Kyjov) in the eastern parts of the Pieniny Klippen Belt (Fig. 7A, ANOSIM, $R = 0.36$, $p < 0.001$). Deposits of the Žiačik section dominated by floatstone and packstone-grainstone are characterized by higher proportions of Fe-stained coatings, dissolved shells, and Fe-stained infills than deposits at the Vršatec and Kyjov sections, represented by floatstone and rudstone (Fig. 7A).

Preservation of Ammonoids

On the scale of several millimeters and centimeters in rudstone, syndepositional shell dissolution expressed by partly dissolved shells and coated molds filled by interstitial micrite is spatially associated with precipitation of radiaxial fibrous calcite and scalenohedral cement within the same ammonoid shells (Fig. 3D). This spatial association between primary cement and dissolved ammonite shells is rare in floatstone. Interstitial micrite can predate as well as postdate the formation of radiaxial fibrous calcite. Proportions of fragmented and bored ammonoids are invariably high, and proportions of encrustation are very low (Figs. 7A–B). In contrast, proportions of Fe-stained coatings, Fe-stained infills, and proportions of shells affected by syndepositional dissolution vary substantially among deposit types (Figs. 7A–B). There is a highly positive and significant relationship between proportions of Fe-stained coatings and proportions of dissolved shells (Spearman $r = 0.73$, $p < 0.0001$) and between proportions of Fe-stained infills and proportions of dissolved shells (Spearman $r = 0.72$, $p < 0.0001$).

Multivariate analyses show moderately high and significant differences in ammonoid alteration among rudstone, floatstone, and packstone-grainstone (ANOSIM $R = 0.4$, $p < 0.001$; see Fig. 8A). Packstone-grainstone highly differs in preservation from rudstone (ANOSIM, $R = 0.92$, $p < 0.001$) and floatstone (ANOSIM, $R = 0.44$, $p = 0.001$). Rudstone and floatstone are more similar but still significantly different (ANOSIM, $R = 0.22$, $p < 0.002$). These three deposit types are dominated by the smallest size class (<1 mm). They do not significantly differ in frequency distribution of size classes (ANOSIM $R = 0.08$, $p = 0.07$), with 45%–60% of ammonoid remnants represented by the size class <1 mm.

Shell-rich rudstone is characterized by low proportions, shell-poor floatstone by moderately high proportions, and packstone-grainstone by the highest proportions of Fe-stained coatings and dissolved shells (Fig. 7B). The proportion of dissolved shells is highly variable but several factors higher in shell-poor floatstone (mean = 0.28) than in shell-rich rudstone (mean = 0.06). The mean dissolved shell volume (i.e., proportion of shells affected by syndepositional dissolution multiplied by shell packing density) is, however, similar between shell-poor (max = 0.07, mean = 0.02) and shell-rich beds (max = 0.09, mean = 0.015).

Effects of Extrinsic and Intrinsic Factors on Ammonoid Preservation

Proportions of cement, micrite, and shells >5 mm significantly explain 36% of variation in taphonomic alteration in canonical analysis of principal coordinates (Fig. 8B) and explain 34%–40% of deviance in the

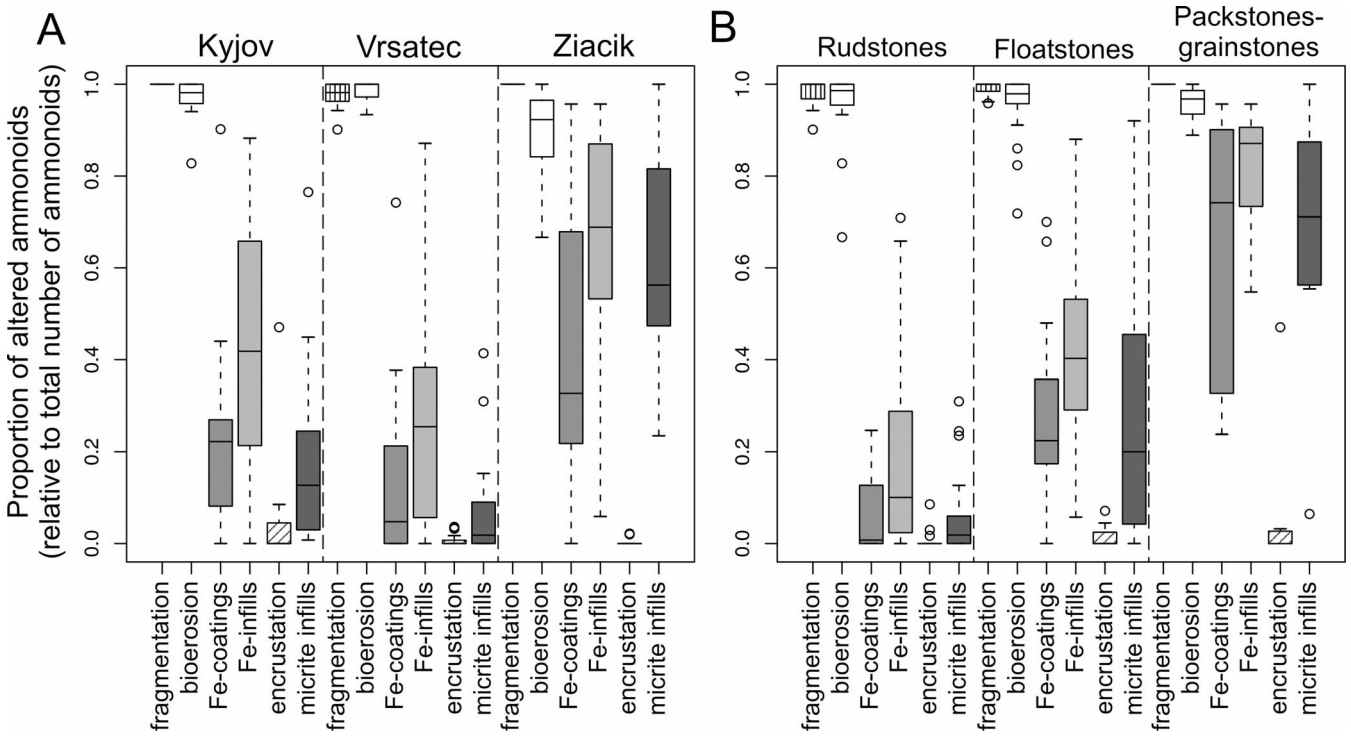

FIGURE 7—Differences in proportions of taphonomic alteration among three sections and three deposit types. A) Deposits at Vršatec characterized by lowest alteration levels; deposits at Žiačik characterized by highest alteration levels, indicating spatial variations in preservation. B) Rudstone characterized by lowest alteration levels and packstone-grainstone characterized by highest alteration levels. Box plots display median, 25, and 75 quartile values; whiskers indicate extreme values (1.5 × the interquartile range); open circles represent outliers.

overall taphonomic alteration in multiple GLM (Table 1). Proportions of cement alone have significant effects on the overall taphonomic alteration, explain a relatively high amount of deviance in simple GLM (Table 1), and have significant effects on taphonomic preservation in CAP (explained variation = 17%, p = 0.005). The relationships between the proportion of cement on one hand and the proportion of Fe-stained coatings and syndepositional dissolution on the other are also significantly negative (Figs. 9A–B, Table 1).

Proportions of micrite have insignificant effects on the overall taphonomic alteration in CAP and in simple GLM (Figs. 9C–D, Table 1).

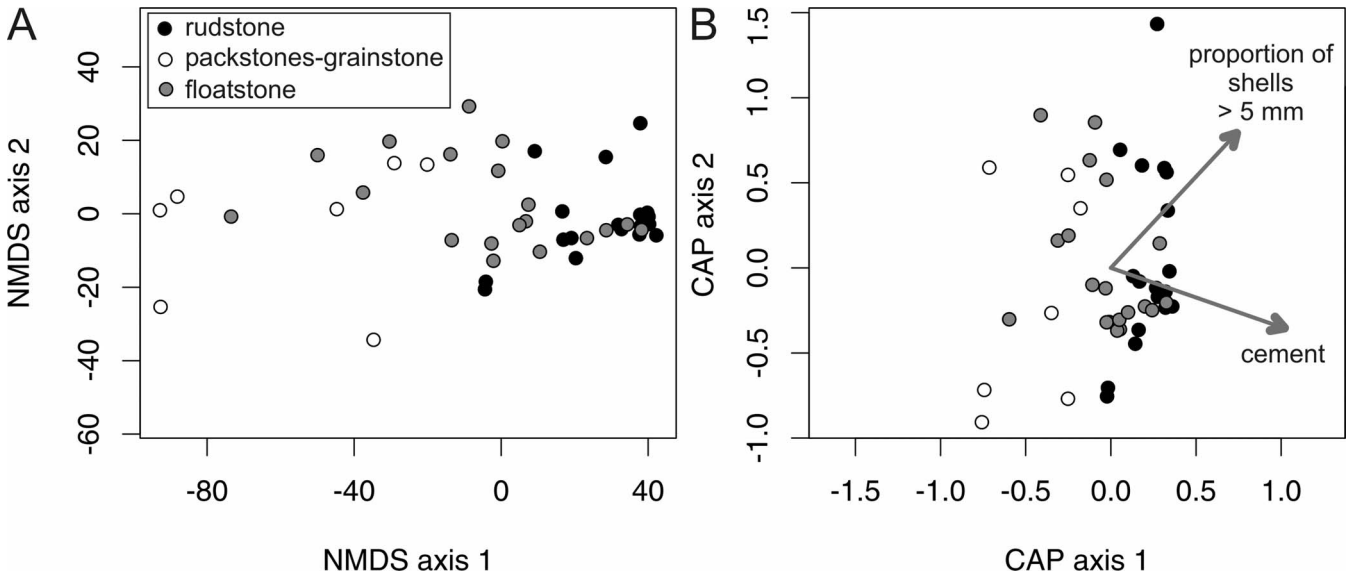

FIGURE 8—Multivariate taphofacies analyses. A) Nonmetric multidimensional scaling (NMDS) ordination of 44 samples based on six taphonomic variables and the Manhattan distance shows a partial segregation among three deposit types. B) Proportion of cement and proportion of shells >5 mm (relative to total number of shells) have significant effects on taphonomic preservation (expressed by six taphonomic variables) in the canonical analysis of principal coordinates (CAP). The proportion of micrite has insignificant effects on the overall taphonomic alteration. Vectors of the two predictor variables originate at the centroid of the multivariate space, and arrows point to the direction of most rapid change in that variable.

TABLE 1—Simple and multiple generalized linear models evaluating statistical effects of cement, micrite, and proportion of shells >5 mm on (1) overall taphonomic alteration (first NMDS axis), (2) proportion of Fe-stained shells, and (3) proportion of shells affected by syndepositional dissolution. NMDS = nonmetric multidimensional scaling.

	Slope	Standard error	t-test	p-value
Response variable—overall alteration (NMDS axis 1)				
Cement (dev. explained = 0.19)	−0.66	0.21	−3.05	0.004
Micrite (dev. explained = 0.04)	−0.26	0.19	−1.34	0.19
Proportion of shells >5 mm (dev. explained = 016)	−0.59	0.21	−2.82	0.0074
Cement + micrite + shell size (dev. explained = 0.4)				
Cement	−0.81	0.24	−3.36	0.0018
Micrite	−0.65	0.19	−3.26	0.0023
Proportion of shells >5 mm	−0.25	0.22	−1.12	0.27
Response variable—proportion of Fe-stained coatings				
Cement (dev. explained = 0.2)	−0.77	0.26	−2.95	0.0052
Micrite (dev. explained = 0.05)	−0.33	0.22	−1.5	0.14
Proportion of shells >5 mm (dev. explained = 0.15)	−0.65	0.25	−2.6	0.013
Cement + micrite + shell size (dev. explained = 0.4)				
Cement	−0.92	0.28	−3.32	0.0019
Micrite	−0.71	0.22	−3.3	0.002
Proportion of shells >5 mm	−0.22	0.26	−0.88	0.38
Response variable—proportion of dissolved shells				
Cement (dev. explained = 0.18)	−0.82	0.29	−2.8	0.0077
Micrite (dev. explained = 0.03)	−0.28	0.25	−1.15	0.26
Proportion of shells >5 mm (dev. explained = 0.15)	−0.73	0.29	−2.53	0.015
Cement + micrite + shell size (dev. explained = 0.34)				
Cement	−0.92	0.33	−2.77	0.0085
Micrite	−0.67	0.26	−2.63	0.012
Proportion of shells >5 mm	−0.31	0.31	−0.99	0.33

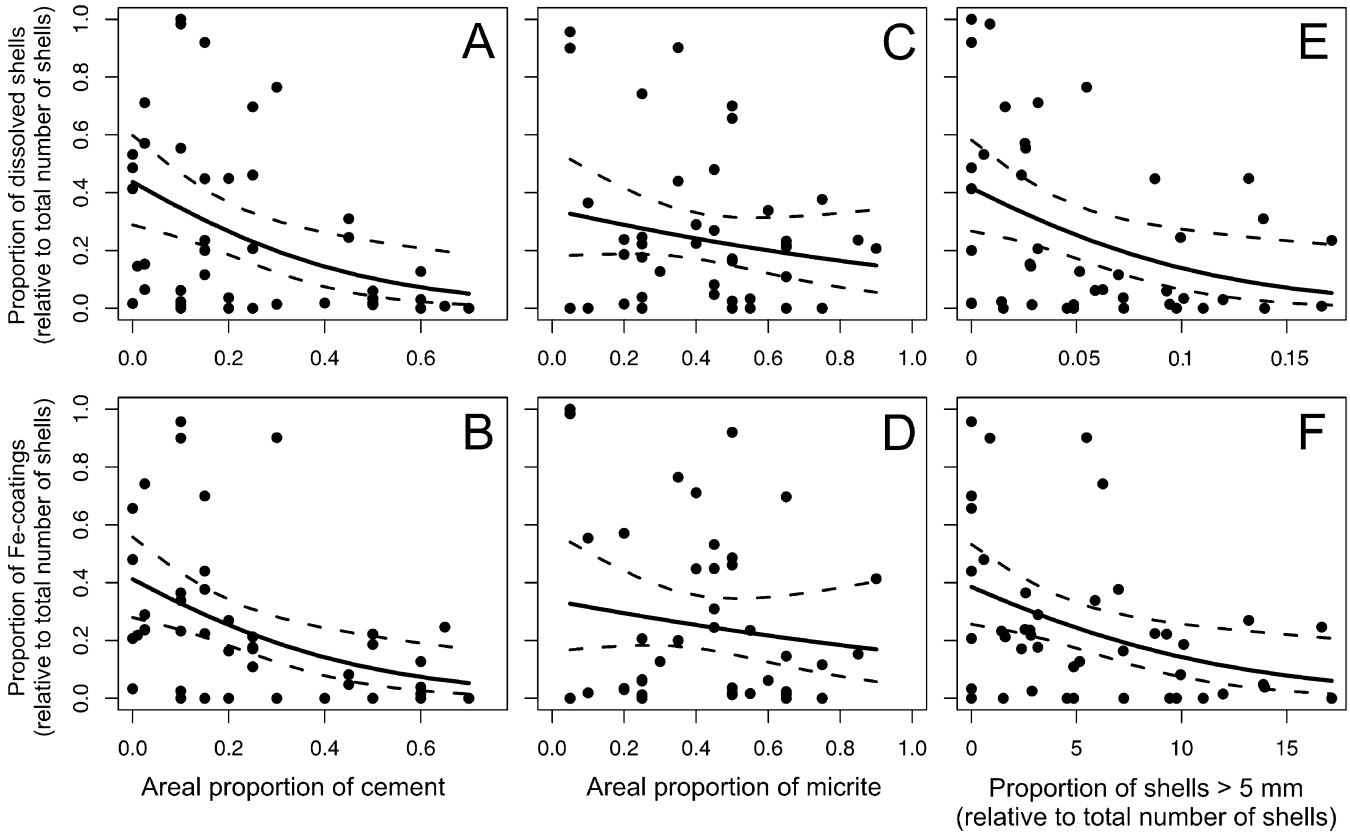

FIGURE 9—Simple generalized linear models showing significantly negative effects of cement (A–B), insignificant effects of micrite (C–D), and significantly negative effects of the proportions of shells >5 mm on taphonomic alteration (E–F), expressed by proportions of syndepositional dissolution and proportions of Fe-stained coatings. Error bars (dashed lines) are 95% confidence intervals.

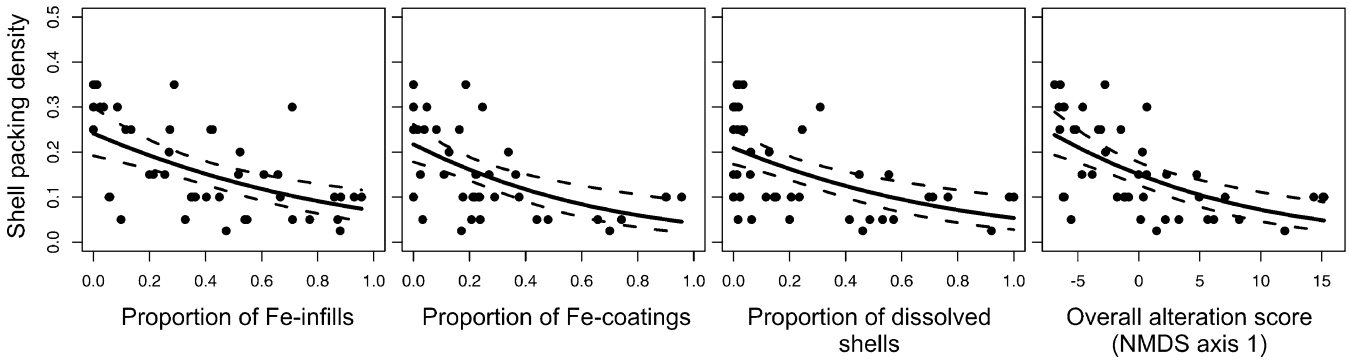

FIGURE 10—Generalized linear models showing significantly negative statistical effects of three alteration variables (proportions of ammonoid shells with Fe-stained infills, Fe-stained coatings, and syndepositional dissolution) and of the overall taphonomic alteration on ammonoid shell-packing density demonstrate that variations in shell abundances are related to variations in production and destruction rate. NMDS = Nonmetric multidimensional scaling.

Proportions of micrite, however, have significant effects on the overall taphonomic alteration in multiple GLM (slope = −0.58, p = 0.002, Table 1). Proportions of shells >5 mm have significant effects on the overall taphonomic alteration in simple GLM (Table 1, Figs. 9E–F). Proportions of shells >5 mm also have significant effects on the overall taphonomic alteration in CAP (explained deviance = 9%, p = 0.036). Note that some factors are highly correlated because proportions of cement correlate significantly positively with proportion of shells >5 mm (Spearman r = 0.58, p < 0.0001) and negatively with proportion of micrite (Spearman r = -0.36, p = 0.02). The effects of cement and shell size are redundant in multiple GLM, and the proportion of shells >5 mm thus does not explain any of the variation in the taphonomic alteration, beyond the variation explained by proportions of cement (Table 1).

Ammonoid Shell-Packing Density

Sedimentation and Shell-Input Rates.—Generalized linear models show significantly negative statistical effects of proportions of fragmentation, Fe-stained coatings, and syndepositional dissolution on ammonoid shell-packing density (Fig. 10, Table 2). Proportions of Fe-stained coatings and syndepositional dissolution have the highest effects on shell-packing density, show comparable slope sizes (−0.43 to −0.49), and explain similar amounts of deviance (about 30%). The overall taphonomic alteration represented by sample scores along the first NMDS axis also has a significantly negative effect on shell-packing density (slope = −0.51). Effects of bioerosion and encrustation on shell-packing density are insignificant (Fig. 10, Table 2). The frequency distribution for shell-packing density is bimodal, with two modes at 0.1 and 0.25 (Fig. 11A).

Durability and Productivity.—The proportion of juveniles and the proportion of ammonitellas are positively rank correlated (r = 0.32, p = 0.036). Notably, the proportion of ammonitellas is not rank correlated with the proportion of cement (r = 0.21, p = 0.17, Fig. 12A), and the proportion of juveniles and shells >5 mm are positively rank correlated with the proportion of cement (r = 0.48, p = 0.001, and r = 0.56, p < 0.0001, respectively; see Figs. 12B–C). The proportion of the smallest-size classes, therefore, does not increase with increasing cement proportions. There are significantly positive and relatively strong statistical effects of cement proportions on ammonoid shell packing density in simple and multiple GLM (slopes = 0.55–0.56; Fig. 13A), the Spearman rank correlation is highly positive (r = 0.78, p < 0.0001), and the median proportion of cement in shell-poor beds is significantly smaller than in shell-rich deposits (Wilcoxon test, p < 0.0001; Fig. 11A).

The abundance of ammonoid embryonic stages measured by the proportion of ammonitellas relative to total plankton density has significantly positive effects on shell-packing density in simple GLM (Fig. 13B, slope = 0.25, p = 0.03; Table 3). The Spearman rank correlation and partial rank correlation between shell-packing density of ammonoids and the proportion of ammonitellas, however, are positive but insignificant, and the difference in the median proportion of ammonitellas between shell-poor and shell-rich deposits is insignificant (Wilcoxon test, p = 0.17; Fig. 11B).

The proportion of early juveniles has significantly positive effects on ammonoid shell-packing density in simple GLM (Fig. 13C, slope = 0.32, p = 0.001). The Spearman rank correlation between the proportion of juveniles and shell-packing density is significantly positive (r = 0.58, p < 0.0001), and median proportion of early juveniles is significantly smaller in shell-poor than in shell-rich deposits (Wilcoxon test, p < 0.0001; Fig. 11B). Partial rank correlation between the proportion of juveniles and shell-packing density, controlling for the effects of cement, is also significantly positive (partial r = 0.38, p = 0.009). Neither the proportion of ammonitellas nor the proportion of juveniles, however, explains a unique portion of deviance in ammonoid shell-packing density in multiple GLM (Table 3).

DISCUSSION

Taphonomic Pathways

Poor sorting of ammonoids in floatstone and rudstone, co-occurrence of large-sized ammonoids with ammonitellas and juveniles, and spatial patchiness of shell concentrations imply that postmortem drift of ammonoids from their living habitats was not extensive; shell concentrations represent parautochthonous assemblages. Imbricated and convex-up oriented ammonoid shells and fragments filled with laminated and graded sediment and sharp bases of rudstones indicate that their deposition was episodically affected by high-energy currents. Orientation of finely laminated internal sediment in intraskeletal pores of rudstone, however, demonstrates that bioturbation did not displace and currents did not reorient shells. High proportions of bioerosion imply that shells were not immediately buried or cemented after their death—they do not represent rapidly accumulated single-event concentrations of cephalopod shells.

Abundant intraclasts, bored ammonoid molds, and grading and erosive bases indicate that sea-bottom disturbance and reworking were locally high also during deposition of floatstone. The presence of exhumed molds and intraclasts but absence of truncated (faceted) shells (e.g., Fernández-Lopéz and Meléndez, 1994) implies that floatstone sediment was semiconsolidated rather than completely lithified. Floatstone and rudstone thus likely correspond to environments with low-to-moderate-intensity bottom currents, and crinoidal packstones and grainstones correspond to conditions of long-term winnowing, reworking, and sorting in high-energy environments. Poorly preserved ammonoids in packstone and grainstone probably underwent several phases of syndepositional dissolution and cementation owing to long-term sediment reworking and winnowing.

Multivariate analyses show that the increase in proportions of Fe-stained coatings, encrustation, and syndepositional dissolution proceeds

TABLE 2—Generalized linear models evaluating statistical effects of six taphonomic variables (proportions of altered shells) and of overall taphonomic alteration (first NMDS axis) on shell-packing density of ammonoids (excluding ammonitellas and early juveniles). NMDS = nonmetric multidimensional scaling.

	Slope	Standard error	t-test	p-value	Dev. explained
Response variable—ammonoid shell packing density					
Proportion of fragmented shells	−0.26	0.09	−2.89	0.006	0.155
Proportion of bored shells	0.23	0.14	1.7	0.1	0.075
Proportion of shells with Fe-infills	−0.43	0.1	−4.12	0.00018	0.300
Proportion of Fe-stained shells	−0.49	0.12	−3.96	0.00028	0.299
Proportion of dissolved shells	−0.46	0.12	−3.93	0.0003	0.294
Proportion of encrusted shells	−0.13	0.15	−0.9	0.38	0.023
Overall alteration—NMDS axis 1	−0.51	0.11	−4.44	<0.0001	0.347

from rudstone to floatstone and packstone-grainstone. Relationships among taphonomic variables imply that the preservation of ammonoids of the Dursztyn Formation was related initially to rapid postmortem fragmentation and bioerosion when exposed on sediment-water interface. Bioerosion rate was probably high and preceded formation of Fe-stained coatings based on consistently high proportions of borings filled with iron coatings. Rapid fragmentation and bioerosion processes were followed by either (1) formation of Fe-stained coatings and thin multilayered microbial crusts, and subsequent syndepositional dissolution in bioturbated floatstone (followed by repeated exhumation and burial events), or (2) reduced rate of syndepositional shell dissolution and subsequent cement precipitation in intraskeletal and shelter pores in rudstone. Proportions of dissolved moldic shells indicate that, on average, less than 30% of ammonoids were dissolved in a semilithified mixed layer in shell-poor sediment and less than 10% of ammonoids were dissolved in shell-rich sediments. Note that the syndepositional cementation rate in present-day aphotic deep-shelf and slope environments—in environments comparable in depth to those at the Czorsztyn Ridge pelagic carbonate platform—can occur very rapidly on the scale of several months and years (Grammer et al., 1993, 1999), and deep-shelf carbonate cements can form extensive crusts under greenhouse-type depositional conditions (Milliman et al., 1969; Brachert, 1999).

Effects of Dissolution-Cementation versus Effects of Exposure Time

The close spatial association of dissolved aragonite and precipitated calcite within ammonoid shells in shell-rich deposits implies simultaneous coupling in dissolution of unstable phases and subsequent precipitation of less-soluble phases and points to the role of aragonite in providing the source for precipitation of cement (e.g., Knoerich and Mutti, 2006). This association is probably conditioned by high input of aragonite shells because it is observed rarely in shell-poor floatstone. Syndepositional dissolution of aragonite shells took place in shallow depths because micrite infillings of dissolved shell walls are continuous with interstitial micrite in intraskeletal voids (see Figs. 3C–D). Early cementation and sediment consolidation are also documented by the presence of exhumed and bored bioclasts filled with internal micrite and by the presence of microscopic firmgrounds. Preservation of dissolved shells subsequently replaced by calcite was, therefore, controlled by semiconsolidated sediment firmness: aragonite dissolution in soft sediment leaves no molds or ghosts (e.g., James et al., 2005).

The positive relationship between cementation and low rates of destruction of individual ammonoid shells is also supported by analyses that show large and negative statistical effects of cement on proportions of ammonoid shells affected by syndepositional dissolution. Semilithified sediment and high proportions of cement that fills voids directly imply pore-water chemistry that can diminish loss of individual aragonite shells owing to syndepositional dissolution (e.g., Fig. 3E). Such early diagenetic combination of aragonite dissolution, sediment infiltration, and cement precipitation occurred also in other environments on pelagic carbonate platforms (Aubrecht et al., 2002; Neuweiler and Bernoulli, 2005).

High abundance of micrite can decrease rates of formation of Fe-staining owing to sediment veneers that cover shell surfaces, and abundance of micrite can negatively correlate with the length of exposure time at sediment-water interface (Davies et al., 1989; Lescinsky et al., 2002). Statistical effects of micrite on ammonoid preservation are relatively small, however. Taphonomic alteration of ammonoids in the Dursztyn Formation was affected most likely by local variations in pore-water chemistry, rather than by variations in the length of exposure time of ammonoids on sediment-water interface. This pattern partly contrasts with other environments where changes in net-sedimentation rate and correlated bathymetric changes have substantial effects on ammonoid preservation (Fernández-Lopéz and Melendez, 1995; Caracuel et al., 2000; Fernández-Lopéz, 2000; Fernández-Lopéz et al., 2002; Olóriz et al., 2002, 2004). Variations in environmental factors that affect variations in the length of exposure time are partly captured by differences between grainstone-packstone on one hand and floatstone and rudstone on the other hand, but ammonoid preservation also substantially depends on local variations in pore-water chemistry and in production rates of shell producers. Powell et al. (2008) similarly show that preservation of mollusks in modern shelf and slope carbonate environments are also strongly linked to local site-specific edaphic factors rather than to large-scale bathymetric gradients.

Sedimentation versus Ammonoid Shell-Input Rates

Variations in ammonoid abundance in shell concentrations is mostly explained in terms of a reduced net-sedimentation rate owing to changes in hydrodynamic activity or proximity of sediment input (Martire, 1992; Santantonio, 1993; Martire and Pavia, 1996; Fernández-Lopéz et al., 2002). For example, ammonoid-rich and aptychi-rich layers that alternate with barren beds in the Upper Jurassic succession of Mexico were interpreted as temporal changes in selective sorting, transport, and secondary enrichment of ammonoid shells owing to changes in current regime (Olóriz et al., 1997). The variations in ammonoid abundances on pelagic carbonate platforms during the Kimmeridgian–Berriasian, however, are unlikely related to reduced sedimentation but correspond to variations in shell production and destruction rates because taphonomic alteration associated with condensed sedimentation has negative, rather than positive, effects on shell-packing density (Tomašových et al., 2006).

Reduced sedimentation rates, however, might covary with an increase in shell packing density when reduced sedimentation rates do not increase assemblage-level taphonomic alteration. For example, variations in net-sedimentation rate owing to changes in winnowing can be coupled with variations in cementation rate because a flux of seawater through sediment pores can be enhanced when concentrations of shells are present at sediment-water interface (Martire, 1992). In this case, dissolution rates are expected to be reduced with decreasing sedimentation rate. In addition, hydrodynamic activity and sediment winnowing near topographic breaks can be coupled with increased food supply and, thus, support higher production rates of biomass (Santantonio, 1993). The spatial reduction in shell-packing density between the highly condensed Vršatec 1

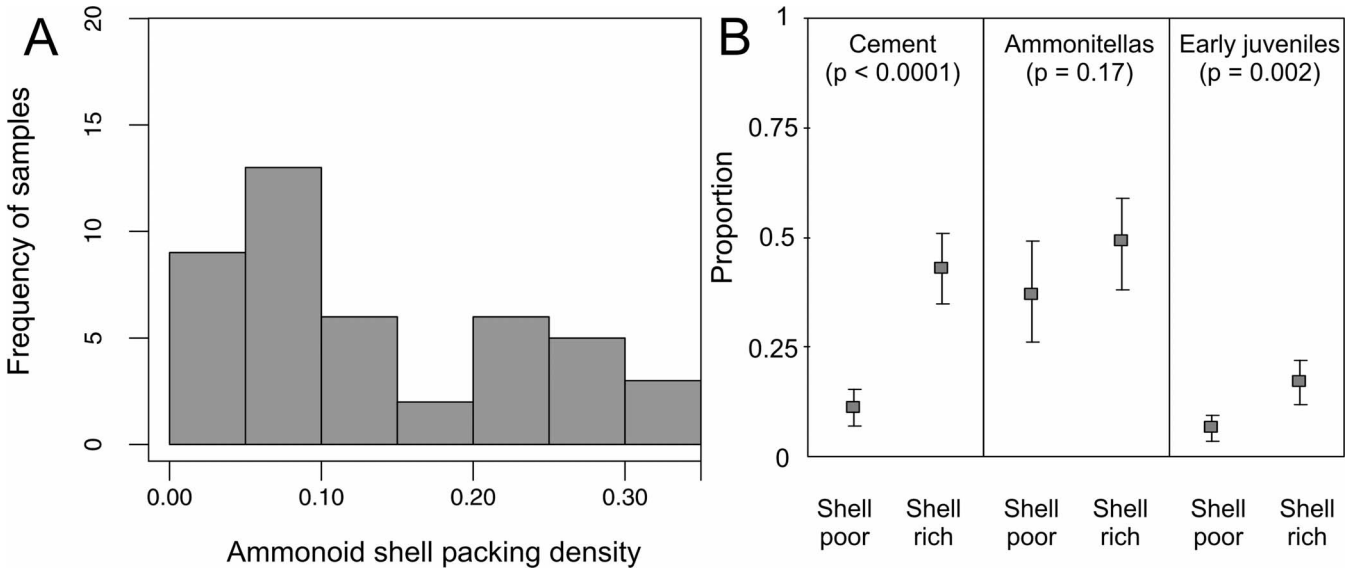

FIGURE 11—Analyses of shell packing density. A) Bimodal frequency distribution of shell-packing density (median density = 0.125). B) Differences in proportion of cement, ammonitellas (relative to total plankton density), and early juveniles (relative to total number of ammonoid individuals) between shell-poor (shell-packing density < 0.125) and shell-rich deposits (shell-packing density > 0.125). Error bars (dashed lines) are 95% confidence intervals.

section with rare rudstone and the thicker Vršatec 2 section with common rudstone, however, demonstrates that the increase in the frequency and thickness of shell concentrations opposes the decrease in net-sedimentation rate.

Ammonoid Destruction Rates

Negative statistical effects of cement on the overall taphonomic alteration, positive effects of cement on shell-packing density, and also negative effects of the overall taphonomic alteration on ammonoid shell-packing density indicate that variations in shell abundance are strongly related to variations in shell destruction rates and, thus, to seafloor and marine-burial diagenetic processes of cementation that can reduce destruction rates. Proportions of dissolved shells demonstrate that the syndepositional dissolution rate of individual ammonoid shells was more reduced in shell-rich than in shell-poor sediments.

High input of aragonitic shells, leading to high shell-packing density on the seafloor, can promote cement formation and decrease rate of destruction via three mechanisms: (1) dissolution of less-stable aragonitic shells can be a significant source releasing bicarbonate ions that buffer alkalinity and enhance slow precipitation of less-soluble calcite in shell-rich rudstone (Boudreau and Canfield, 1993; Neuweiler and Bernoulli, 2005), (2) shell concentrations enhance sediment porosity and, thus, increase mixing of sediment pore waters in the taphonomically active zone with the ambient oversaturated seawater (Kidwell, 1986, 1989; Tucker and Wright, 1990; Palmer and Wilson, 2004), and (3) shell concentrations can increase sediment stability and decrease bioturbation, thus favoring precipitation of cements (Macintyre, 1977, 1984). The bimodal frequency distribution of ammonoid shell-packing density indeed indicates a specific threshold in shell packing that is necessary for cementation in rudstone. These mechanisms can provide an important positive feedback between high shell-packing density and the low rate of shell dissolution and can enhance preservation of ammonoids by creating favorable pore-water chemistry.

The close association of dissolved ammonoid shells and precipitated cement seen in thin sections of rudstone (Fig. 3E) indicates that a local source for cement was at least partly derived from dissolution of ammonoid shells. The source of calcite cement in carbonate rhythmites is mainly assigned to variations in input of periplatform aragonite mud (Munnecke and Westphal, 2005), but shallow carbonate factories were probably lacking or limited in extent on pelagic carbonate platforms in the Pieniny Klippen Belt. Although the possibility of other aragonitic sources is not excluded, high abundance of ammonoid shells points to

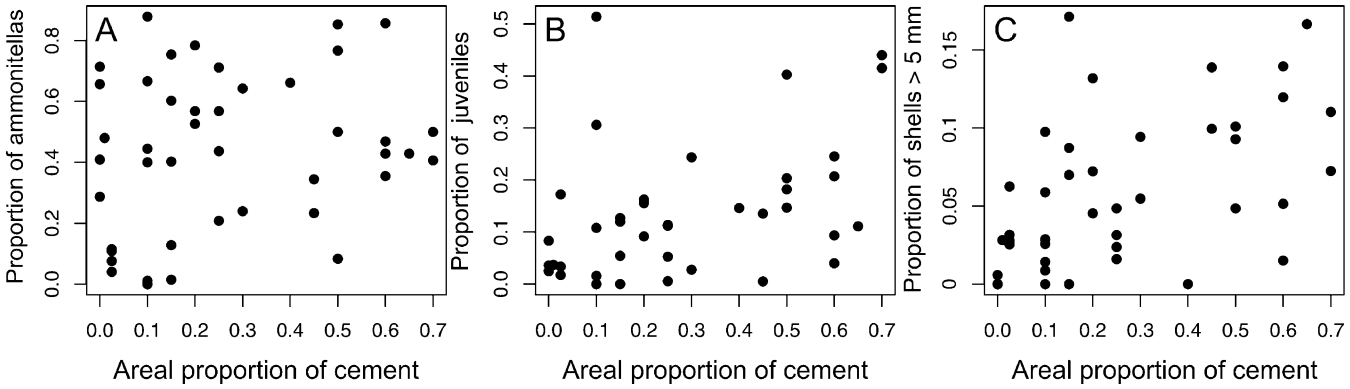

FIGURE 12—Bivariate relationships between proportions of three size classes and proportions of cement show that the preservation potential of the smallest-size classes does not increase with increasing proportions of cement. A) Insignificant relationship between proportion of ammonitellas and proportions of cement (Spearman r = 0.21, p = 0.17). B) Significantly positive relationship between the proportion of early juveniles and proportions of cement (Spearman r = 0.48, p = 0.001). C) Significantly positive relationship between the proportion of shells >5 mm and proportions of cement (Spearman r = 0.56, p = 0.0001).

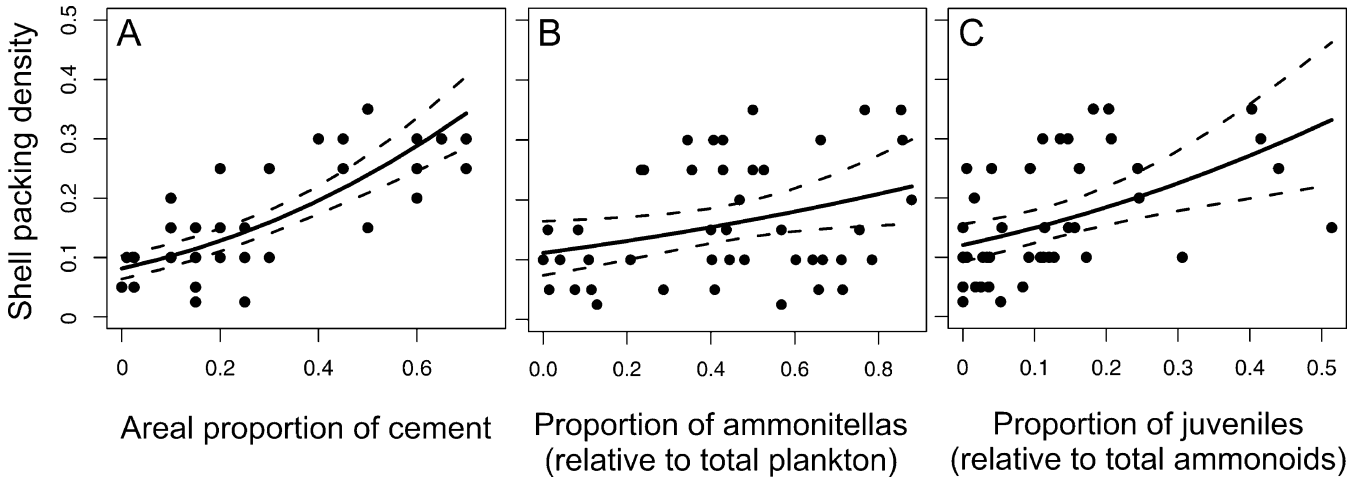

FIGURE 13—Simple generalized linear model evaluating statistical effects of durability and productivity indicators on ammonoid shell-packing density, excluding ammonitellas and early juveniles. A) Significantly positive effects of cement indicate that variations in shell-packing density are related to variations in shell-destruction rates. B) Significantly positive effects of proportions of ammonitellas suggest that the increase in shell-packing density is related to the increase in fecundity. C) Significantly positive effects of proportions of early juveniles imply that the increase in shell-packing density is coupled with the increase in juvenile mortality. Error bars (dashed lines) are 95% confidence intervals.

ammonoids as providing substantial amount of bicarbonate for cement formation (see also Sanders, 2001; Wright et al., 2003; Wheeley et al., 2008).

In the mechanism in which ammonoid dissolution leads to the porewater excess of bicarbonate ions and buffers the carbonate saturation state (e.g., Walter et al., 1993; Andersson et al., 2003), and subsequently reduces dissolution rates and enhances cementation (Palmer and Wilson, 2004), it is predicted that dissolution rates of individual shells are lower in shell-rich than in shell-poor deposits (as observed in this study). This mechanism also predicts that the total amount of dissolved aragonite is higher during the peaks of ammonoid shell input than during shell-poor intervals because the dissolution rate will not decrease if the total amount of released bicarbonate does not increase from shell-poor to shell-rich beds (keeping background organic matter decomposition constant). It should be noted that, although the proportion of dissolved ammonoid shells is lower in shell-rich than in shell-poor beds, shell-rich beds still consist of relatively high number of moldic (dissolved) shells. The second prediction, assuming a relatively closed diagenetic system, is not fully in accord with observations because the dissolved shell volume (i.e., the proportion of shells affected by syndepositional dissolution multiplied by shell-packing density) is comparable between shell-poor and shell-rich beds. This estimate of dissolved shell volume, however, is still conservative because it refers to the amount of (moldic) dissolved shells in semiconsolidated sediment. This diagenetic system was probably more open in coarse-grained rudstone than in mud-rich floatstone, and the true amount of dissolved aragonite was thus likely higher in shell-rich beds relative to shell-poor beds.

Signs of syndepositional dissolution in cohesive sediment indicate that dissolution-dominated pathways, not buffered by high input of aragonitic shells, were located in the semilithified mixed layer prone to sediment turnover and bioturbation. Bioturbation in the topmost sediment layers generally favors syndepositional dissolution by increasing acid production owing to organic matter oxidation (Archer, 1991; Walter et al., 1993). Although alkalinity returns to saturation or supersaturation downcore in the zone of final burial (e.g., Walter and Burton, 1990; Ku et al., 1999), bioturbated layers have reduced alkalinity relative to the overlying seawater in the absence of high water-exchange rates (Tucker and Wright, 1990). Sulphide oxidation in Fe-poor carbonate sediments can also enhance dissolution because iron oxides can buffer free sulphides to low levels in pore waters by permitting pyrite formation (Ku et al., 1999; Perry and Taylor, 2006). Pyrite grains are very rare in floatstone, and, in spite of their red color, concentrations of dispersed iron hydroxides can be still generally low (Préat et al., 2006; but see van der Kooij et al., 2007). Fe-stained coatings that form biofilms and thin microbial crusts are probably related to the activity of Fe-oxidizing bacteria and fungi that inhabit dyserobic conditions within the taphonomically active zone (Préat et al., 2006; Mamet and Préat, 2006).

Ammonoid Production Rates

Nonrandom relationships between shell-packing density of large ammonoids on one hand and proportions of ammonitellas and early juveniles on the other imply that high abundance of ammonoid shells in the Dursztyn Formation reflect time intervals of truly high ammonoid production rates. The differential diagenesis model can, however, bias variations in absolute abundances of fossils in carbonate sequences with variations in cementation and can be indistinguishable from differential productivity models (Westphal et al., 2000). Early diagenetic processes accompanied by dissolution and redistribution of calcium carbonate can lead to an apparent increase in proportions of ammonitellas and early juveniles (relative to larger shells) because higher cementation can enhance preservation of small shells. Higher abundance of ammonitellas and juveniles in deposits with higher shell-packing densities is not a spurious consequence of enhanced preservation of small-sized shells owing to higher cementation rates because (1) proportions of small shells and fragments, relative to larger shells, do not increase with increasing cementation, (2) size-frequency distributions of ammonoid shells and fragments are not significantly different among the three deposit types, and (3) partial Spearman rank correlations between shell-packing density and proportion of early juveniles that controls for the effects of cement is significantly positive.

The effect sizes of proportions of ammonitellas and early juveniles are small relative to the effects of durability in simple GLM (Table 3). Shell-packing density and abundances of ammonitellas and early juveniles measured at the centimeter scale in thin section can be affected by high spatial heterogeneity. Such spatial patchiness can cause peaks in abundances of ammonitellas, juveniles, and adults that are spatially separated at small scales, even when abundances of individual age classes are positively correlated at larger spatial scale. In addition, small eggs and hatchlings can likely be subjected to substantial passive drift by water masses, leading to additional heterogeneity at small spatial scales (Waluda et al., 2001, González et al., 2005). The positive relationship between abundance of ammonitellas, juveniles, and adult ammonoids qualitatively occurs also at regional scales, however. Ammonitellas and large-sized ammonoids are

TABLE 3—Generalized linear models evaluating statistical effects of durability (cement) and productivity indicators (proportions of ammonitellas and proportions of early juveniles) on shell-packing density of ammonoids (excluding ammonitellas and early juveniles).

	Slope	St. error	t-test	p-value
Response variable—shell packing density				
Cement (dev. explained = 0.61)	0.56	0.07	8.1	<0.0001
Ammonitellas (dev. explained = 0.1)	0.25	0.11	2.24	0.03
Juvenile ammonites (dev. explained = 0.23)	0.32	0.09	3.56	0.001
Cement + ammonitella/plankton ratio (dev. explained = 0.64)				
Cement	0.54	0.069	7.88	<0.0001
Ammonitellas (relative to total plankton)	0.14	0.075	1.9	0.06
Cement + early juveniles (dev. explained = 0.62)				
Cement	0.5	0.079	6.37	<0.0001
Early juveniles (relative to total ammonoids)	0.11	0.076	1.43	0.16
Cement + ammonitella/plankton ratio + early juveniles (dev. explained = 0.64)				
Cement	0.5	0.077	6.36	<0.0001
Ammonitellas (relative to total plankton)	0.12	0.08	1.5	0.13
Early juveniles (relative to total ammonoids)	0.09	0.077	1.1	0.28

abundant components in deposits originating in shallow habitats of the Czorsztyn Ridge only. In contrast, the planktonic crinoid *Saccoccoma*, radiolarians, planktonic green algae, and calpionellids were rock-forming microcomponents during the Kimmeridgian–Berriasian interval in slope and basinal environments adjacent to the Czorsztyn Ridge (Reháková, 2000).

Variations in abundances of ammonitellas can be either a consequence of increased embryonic mortality (keeping the number of produced eggs constant) or directly caused by increased fecundity (keeping embryonic mortality constant). The first scenario, however, should lead to negative correlation between abundances of ammonitellas and the packing density of large-sized ammonoids, assuming a relatively constant size-frequency distribution of ammonoid populations over the period of the time averaging. Thus, variations in abundance of ammonitellas can correspond to an increase in fecundity because they show a positive relationship to the shell-packing density of larger ammonoids (e.g., Figs. 1B, 1D). For example, the fecundity of cephalopods can be affected by variations in prey (food) supply because the gonad size, the amount of yolk in the eggs, and the duration of spawning depend on the food supply (Laptikhovsky and Nigmatulin, 1993). The relationship between the abundances of ammonitellas and shell-packing density needs to be further tested owing to the less conclusive results based on the Spearman rank and Wilcoxon tests.

The positive relationship between proportion of early juveniles and shell-packing density is diagnostic for scenarios in which the increase in ammonoid production rates is coupled with increasing early juvenile mortality, rather than with a decrease in juvenile mortality (Fig. 1B). The association of high shell-packing density with high mortality of early juveniles can be surprising because variations in abundances of present-day coleoids are commonly positively related to survivorship of juveniles (Forsythe et al., 2001; Jackson and Domeier, 2003; Pecl, 2004), and survivorship of juveniles is especially important for persistence of coleoid populations with nonoverlapping generations. High mortality of early juvenile cephalopods, however, can be related to negative effects of density dependence that may lead to resource exhaustion due to high competition for food among juveniles or to cannibalism (e.g., Agnew et al., 2000; Challier et al., 2006). We thus hypothesize that ammonoids that formed shell concentrations in the Dursztyn Formation probably produced a large number of small but vulnerable embryos and juveniles.

Some present-day cephalopods are characterized by extensive migrations between feeding and spawning grounds (Waluda et al., 2001; Moltschaniwskyj and Steer, 2004). Our analyses thus depend on the assumption that variations in ammonoid abundance preserved in the Dursztyn Formation reflect their life history in environments where feeding and spawning grounds are not spatially separated or can be segregated over short intervals but become averaged over longer temporal durations. Extensive migrations are unlikely because ammonoid species found in shell concentrations in the Dursztyn Formation mainly are found near pelagic carbonate platforms of the Western Tethys and are generally rare in other provinces.

Spatial and Temporal Variations in Ammonoid Preservation

High spatial variations in shell-packing density across several meters and across several hundreds of meters indicate that simple space-homogeneous models do not explain the genesis of ammonoid shell concentrations. High variations in sediment thickness across several hundreds of meters probably reveal differential topography of platform blocks caused by fault-controlled subsidence (Mišík and Sýkora, 1993; Krobicki, 1996; Aubrecht and Szulc, 2006). It is possible, therefore, that at short spatial scales, topographic variations contribute to high spatial heterogeneity in production and destruction of shell producers (Zempolich, 1993; Martire, 1996). The intensity of bottom currents is generally highest in areas of topographic breaks near elevated blocks, favoring mixing of pore waters in the bioturbated zones with open supersaturated waters and, thus, enhancing cementation rates (e.g., Fürsich et al., 1992; Martire, 1992). The acceleration of water flow velocity in localized portions of a platform and potential presence of vortices and eddies that are associated with topographic breaks may be also favorable for higher retention of ammonoid eggs and juveniles (Diekmann et al., 2006; but see McClain, 2007) and higher recruitment rates and higher consumption rates owing to higher amount of prey that can be captured in flow per unit time (Genin et al., 1986; Sebens, 1987; Genin, 2004). High spatial variation in shell-packing density can thus copy the original sea-bottom topography because topographic breaks can be associated with high zooplankton productivity that can represent targets for ammonoid feeding and spawning grounds, on the one hand, and with high cementation rates, on the other hand. We hypothesize that the formation of ammonoid shell concentrations corresponds to long-term but spatially variable peaks in ammonoid production rates, with subsequent aragonite dissolution buffering the bottom-water chemistry and causing cementation.

CONCLUSIONS

1. Negative statistical effects of taphonomic alteration on the shell-packing density of ammonoids and the spatial decrease in shell-packing density with decreasing sediment thickness support the hypothesis that long-term variations in production and destruction rates controlled variations in abundance of ammonoid shells in concentrations preserved on pelagic carbonate platforms during the Late Jurassic–earliest Cretaceous. Although the potential to form dense shell concentrations is related to reduced background sedimentation, variations in ammonoid shell-packing

density on pelagic carbonate platforms were probably not caused by variations in sedimentation rates.

2. Variations in shell destruction rates—approximated by proportions of altered shells and by proportion of cement—and variations in shell production rates—proportions of embryonic stages and early juveniles—are related to variations in shell-packing density of larger ammonoid shells. Peaks in abundances of ammonitellas and juveniles are not caused by enhanced preservation of small size classes because proportions of large shells, relative to small individuals, increase with increasing cementation.

3. The proportion of cement has the strongest positive statistical effects on shell-packing density. The close spatial association of dissolved aragonite and precipitated calcite within ammonoid shells in shell-rich deposits, the low proportion of dissolved ammonoids in shell-rich beds, and the rarity of cements and abundance of molds in shell-poor beds indicate a positive relationship between the high packing density of aragonite shells and their preservation rate. Proportions of moldic shells imply that $<30\%$ of shells were dissolved in semilithified bioturbated layers in shell-poor beds and $<10\%$ of shells were dissolved in shell-rich beds. Densely packed ammonoid shells probably provide the substantial source of aragonite for cement formation and can enhance water exchange of pore waters with the ambient seawater, which in turn can reduce the rate of ammonoid destruction. We suggest that the ammonoid shell concentrations correspond to peaks in ammonoid production rates, with aragonite dissolution buffering the pore-water chemistry and leading to cement formation.

4. Abundances of ammonitellas and abundances of early juvenile stages covary positively with ammonoid shell-packing density. Simple models show that the positive relationship between juvenile mortality and shell abundance distinguishes the scenario in which increase in fecundity primarily contributes to the high production rate from other scenarios in which reduced juvenile mortality also increases production rate. We hypothesize that high abundance of ammonoid shells corresponds to peaks in fecundity, followed by high early juvenile mortality, with production of a large number of small but vulnerable embryos and juveniles.

ACKNOWLEDGMENTS

We are thankful to Carlton Brett, one anonymous reviewer, and Stephen T. Hasiotis for comments. We also thank Marián Golej for help with the fieldwork and discussions. This research was supported by the Slovakian Scientific Grant Agency (VEGA 0068/08), Slovak Research and Development Agency (APVV 0465-06, APVV 0248-07), and German Science Foundation (Fu 131/26-1). AT also thanks the National Science Foundation, Division of Earth Sciences (EAR-0345897), and the National Oceanic and Atmospheric Administration California Sea Grant Program Urban Oceans for support. This is a contribution to IGCP project 506 ''Marine and non-marine Jurassic: global correlation and major geological events.''

REFERENCES

Adler, P.B., HilleRisLambers, J., and Levine, J.M. 2007, A niche for neutrality: Ecology Letters, v. 10, p. 95–104.

Agnew, D.J., Hill, S., and Beddington, J.R., 2000, Predicting the recruitment strength of an annual squid stock: *Loligo gahi* around the Falkland Islands: Canadian Journal of Fisheries and Aquatic Sciences, v. 57, p. 2479–2487.

Akçakaya, H.R., 1991, A method for simulating demographic stochasticity: Ecological Modelling, v. 54, p. 133–136.

Akçakaya, H.R., Halley, J.M., and Inchausti, P., 2003, Population-level mechanisms for reddened spectra in ecological time series: Journal of Animal Ecology, v. 72, p. 698–702.

Anderson, M.J., and Willis, T.J., 2003, Canonical analysis of principal coordinates: A useful method of constrained ordination for ecology: Ecology, v. 84, p. 511–525.

Andersson, A.J., Mackenzie, F.T., and Ver, L.M., 2003. Solution of shallow-water carbonates: An insignificant buffer against rising atmospheric CO_2: Geology, v. 31, p. 513–516.

Archer, D., 1991, Equatorial Pacific calcite preservation cycles: Production or dissolution: Paleoceanography, v. 6, p. 561–571.

Aubrecht, R., and Szulc, J., 2006, Deciphering of the complex depositional and diagenetic history of a scarp limestone breccia (Middle Jurassic Krasin Breccia, Pieniny Klippen Belt, Western Carpathians): Sedimentary Geology, v. 186, p. 265–281.

Aubrecht, R., Szulc, J., Michalík, J., Schlögl, J., and Wagreich, M., 2002, Middle Jurassic stromatactis mud-mound in the Pieniny Klippen Belt (Western Carpathians): Facies, v. 47, p. 113–126.

Bacelle, L., and Bosellini, A., 1965, Diagrammi per la stime visiva della composizione percentuale nelle rocce sedimentaire: Annali dell'Universita di Ferrara, Scienze Geologiche e Paleontologiche, v. 1, p. 59–62.

Beukema, J.J., and Dekker, R., 2007, Variability in annual recruitment success as a determinant of long-term and large-scale variation in annual production of intertidal Wadden Sea mussels (*Mytilus edulis*): Helgoland Marine Research, v. 61, p. 71–86.

Birkenmajer, K., 1986, Stages of structural evolution of the Pieniny Klippen Belt, Carpathians: Studia Geologica Polonica, v. 88, p. 7–32.

Böhm, F., and Brachert, T.C., 1993, Deep-water stromatolites and *Frutexites* Maslov from the Early and Middle Jurassic of S-Germany and Austria: Facies, v. 28, p. 145–168.

Boudreau, B.P., and Canfield, D.E., 1993, A comparison of closed- and open-system models for porewater pH and calcite-saturation state: Geochimica et Cosmochimica Acta, v. 57, p. 317–334.

Boyle, P.R., and Boletzky, S. von, 1996, Cephalopod populations: Definition and dynamics: Philosophical Transactions of the Royal Society, London: Biological Sciences, v. 351, p. 985–1002.

Boyle, P.R., and Rodhouse, P., 2005, Cephalopods: Ecology and Fisheries: Blackwell Science, Oxford, UK, 452 p.

Brachert, T.C., 1999, Non-skeletal carbonate production and stromatolite growth within a Pleistocene deep ocean (Last Glacial Maximum, Red Sea): Facies, v. 40, p. 211–228.

Brett, C.E., 1998, Sequence stratigraphy, paleoecology, and evolution: Biotic clues and responses to sea-level fluctuations: PALAIOS, v. 13, p. 241–262.

Bucher, H., Landman, N.H., Klofak, S.M., and Guex, J., 1996, Mode and rate of growth in ammonoids, *in* Landman, N., et al., ed., Ammonoid Paleobiology: Topics in Geobiology: vol. 13, Plenum Press, New York, 407–461.

Caracuel, J.E., Monaco, P., and Olóriz, F., 2000, Taphonomic tools to evaluate sedimentation rates and stratigraphic completeness in Rosso Ammonitico facie (epioceanic Tethyan Jurassic): Rivista Italiana di Paleontologia e Stratigrafia, v. 106, p. 353–368.

Cecca, F., 1992, Ammonite habitats in the Early Tithonian of Western Tethys: Lethaia, v. 25, p. 257–267.

Challier, L., Pierce, G.J., and Robin, J.-P., 2006, Spatial and temporal variation in age and growth in juvenile *Loligo forbesi* and relationships with recruitment in the English Channel and Scottish waters: Journal of Sea Research, v. 55, p. 217–229.

Clari, P.A., and Martire, L., 1996, Interplay of cementation, mechanical compaction, and chemical compaction in nodular limestones of the Rosso Ammonitico Veronese (Middle–Upper Jurassic, Northeastern Italy): Journal of Sedimentary Research, v. 66, p. 447–458.

Clarke, K.R., and Green, R.H., 1988, Statistical design and analysis for a ''biological effects'' study: Marine Ecology Progress Series, v. 46, p. 213–226.

Clarke, M.R., 1996, The role of cephalopods in the worldś oceans: General conclusions and the future: Philosophical Transactions of the Royal Society London, ser. B, v. 351, p. 1105–1112.

Coelho, M.L., Stobberup, K.A., OḎor, R., and Dawe, E.G., 1994, Life history strategies of the squid, *Illex illecebrosus*, in the Northwest Atlantic: Aquatic Living Resources, v. 7, p. 233–246.

Conti, M.A., and Monari, S., 1992, Thin-shelled bivalves from the Jurassic Rosso Ammonitico and Calcari a Posidonia Formations of the Umbrian–Marchean Apennine (Central Italy): Paleopelagos, v. 2, p. 193–213.

Dattilo, B.F., 1996, A quantitative paleoecological approach to high-resolution cyclic and event stratigraphy: The Upper Ordovician Miamitown Shale in the type Cincinnatian: Lethaia, v. 28, p. 21–37.

Davies, D. J., Powell, E.N., and Stanton, R.J., Jr., 1989, Relative rates of shell dissolution and net sediment accumulation—A commentary: Can shell beds form by the gradual accumulation of biogenic debris on the sea floor?: Lethaia, v. 22, p. 207–212.

Diekmann, R., Nellen, W., and Piatkowski, U., 2006, A multivariate analysis of larval fish and paralarval cephalopod assemblages at Great Meteor Seamount: Deep-Sea Research I, v. 53, p. 1635–1657.

Doyle, P., and Macdonald, D.I.M., 1993, Belemnite battlefields: Lethaia, v. 26, p. 65–80.

Fernández-Lopéz, S.R., 2000, Ammonite taphocycles in carbonate epicontinental platforms: Georesearch Forum, v. 6, p. 293–300.

Fernández-López, S.R., Henriques, M.H., and Duarte, L.V., 2002, Taphonomy of ammonite condensed associations—Jurassic examples from carbonate platforms of Iberia: Abhandlungen der geologischen Bundesanstalt, v. 57, p. 423–430.

Fernández-López, S.R., and Meléndez, G., 1994, Abrasion surfaces on internal moulds of ammonites as paleobathymetric indicators: Palaeogeography, Palaeoclimatology, Palaeoecology, v. 110, p. 29–42.

Fernández-López, S.R., and Meléndez, G., 1995, Taphonomic gradients in Middle Jurassic ammonites of the Iberian Range (Spain): Geobios, Supplement 1, v. 18, p. 155–165.

Finnegan, S., and Droser, M.L., 2005, Relative and absolute abundance of trilobites and rhynchonelliform brachiopods across the Lower/Middle Ordovician boundary, eastern Basin and Range: Paleobiology, v. 31, p. 480–502.

Finnegan, S., and Droser, M.L., 2008, Reworking diversity: effects of storm deposition on evenness and sampled richness, Ordovician of the Basin and Range, Utah and Nevada, USA: PALAIOS, v. 23, p. 87–96.

Floquet, M., Cecca, F., Mestre, M., Macchioni, F., Guiomar, M., Baudin, F., Durlet, C., and Alméras, Y., 2003, Mortalité en masse ou fossilization exceptionelle? Le cas des gisements d'âge toarcien inférieur et moyen de la région de Digne-Les-Bains (Sud-Est de la France): Bulletin de la Societé Géologique de France, v. 174, p. 159–176.

Forsythe, J.W., Walsh, L.S., Turk, P.E., and Lee, P.G., 2001, Impact of temperature on juvenile growth and age at first egg-laying of the Pacific reef squid *Sepioteuthis lessoniana* reared in captivity: Marine Biology, v. 138, p. 103–112.

Fürsich, F.T., Oschmann, W., Singh, I.B., and Jaitly, A.K., 1992, Hardgrounds, reworked concretion levels and condensed horizons in the Jurassic of western India: Their significance for basin analysis: Journal of Geological Society, London, v. 149, p. 313–331.

Garrison, R.E., and Fisher, A.G., 1969, Deep-water limestones and radiolarites of the Alpine Jurassic: SEPM (Society for Sedimentary Geology) Special Publications, v. 14, p. 20–56.

Genin, A., 2004, Bio-physical coupling in the formation of zooplankton and fish aggregations over abrupt topographies: Journal of Marine Systems, v. 50, p. 3–20.

Genin, A., Dayton, P.K., Lonsdale, P.F., and Spiess, F.N., 1986, Corals on seamount peaks provide evidence of current acceleration over deep-sea topography: Nature, v. 322, p. 59–61.

Gerhardt, S., and Henrich, R., 2001, Shell preservation of *Limacina inflata* (Pteropoda) in surface sediments from the Central and South Atlantic Ocean: A new proxy to determine the aragonite saturation state of water masses: Deep-Sea Research I, v. 48, p. 2051–2071.

Gómez, J.J., and Fernández-Lopéz, S., 1994, Condensation processes in shallow platforms: Sedimentary Geology, v. 92, p. 147–159.

González, A.F., Otero, J., Guerra, A., Prego, R., Rocha, F.J., and Dale, A.W., 2005, Distribution of common octopus and common squid paralarvae in a wind-driven upwelling area (Ria of Vigo, northwestern Spain): Journal of Plankton Research, v. 27, p. 271–277.

Grammer, G.M., Crescini, C.M., McNeill, D.F., and Taylor, L.H., 1999, Quantifying rates of syndepositional marine cementation in deeper platform environments—New insight into a fundamental process: Journal of Sedimentary Research, v. 69, p. 202–207

Grammer, G.M., Ginsburg, R.N., Swart, P.K., McNeill, D.F., Jull, A.J.T., and Prezbindowski, D.R., 1993, Rapid growth rates of marine aragonitic cements in steep marginal slope deposits, Bahamas and Belize: Journal of Sedimentary Petrology, v. 63, p. 983–989.

Hardie, L.A., 1996, Secular variation in seawater chemistry: An explanation for the coupled secular variation in the mineralogies of marine limestones and potash evaporites over the past 600 m.y.: Geology, v. 24, p. 279–283.

Hendry, J.P., 1993, Calcite cementation during bacterial manganese, iron and sulphate reduction in Jurassic shallow marine carbonates: Sedimentology, v. 40, p. 87–106.

Holland, S.M., and Patzkowsky, M.E., 2007, Gradient ecology of a biotic invasion: Biofacies of the type Cincinnatian series (Upper Ordovician), Cincinnati, Ohio region, USA: PALAIOS, v. 22, p. 392–407.

Jackson, G.D., and Domeier, M.L., 2003. The effects of an extraordinary El Niño/La Niña event on the size and growth of the squid *Loligo opalescens* off Southern California: Marine Biology, v. 142, p. 925–935.

James, N.P., Bone, Y., and Kyser, T.K., 2005, Where has all the aragonite gone? Mineralogy of holocene neritic cool-water carbonates, southern Australia: Journal of Sedimentary Research, v. 75, p. 454–463.

Jenkyns, H.C., 1971, The genesis of condensed sequences in the Tethyan Jurassic: Lethaia, v. 4, p. 327–352.

Kendall, A.C., 1985, Radiaxial fibrous calcite: A reappraisal, *in* Schneidermann, N., and Harris, P.M., eds., Carbonate Cements: Society of Economic Paleontologists and Mineralogists Special Publications, v. 36, p. 59–77.

Kidwell, S.M., 1986, Models for fossil concentrations: Paleobiologic implications: Paleobiology, v. 12, p. 6–24.

Kidwell, S.M., 1989, Stratigraphic condensation of marine transgressive records: Origin of major shell deposits in the Miocene of Maryland: Journal of Geology, v. 97, p. 1–24.

Kidwell, S.M., 1991, The stratigraphy of shell concentrations, *in* Allison, P.A., and Briggs, D.E.G., eds., Taphonomy: Releasing the Data Locked in the Fossil Record: Topics in Geobiology: vol. 9, Plenum Press, New York, p. 115–129.

Kidwell, S.M., and Brenchley, P.J., 1994, Patterns in bioclastic accumulation through the Phanerozoic: Changes in input or destruction?: Geology, v. 22, p. 1139–1143.

Kim, S.-H., and Yi, S.V., 2007, Understanding relationship between sequence and functional evolution in yeast proteins: Genetica, v. 131, p. 151–156.

Klöcker, R., Ganssen, G., Jung, S.J.A., Kroon, D., and Henrich, R., 2006, Late Quaternary millennial-scale variability in pelagic aragonite preservation off Somalia: Marine Micropaleontology, v. 59, p. 171–183.

Knoerich, A.C., and Mutti, M., 2006, Epitaxial calcite cements in Earth history: A cooler-water phenomenon during aragonite-sea times? *in* Pedley, H.M., and Carannante, G., eds., Cool-water carbonates: Depositional systems and palaeoenvironmental controls: Geological Society, London, Special Publications, v. 255, p. 323–335.

Kowalewski, M., 1996, Time-averaging, overcompleteness, and the geological record: Journal of Geology, v. 104, p. 317–326.

Kranz, P.M., 1977, A model for estimating standing crop in ancient communities: Paleobiology, v. 3, p. 415–421.

Krobicki, M., 1994, Stratigraphic significance and palaeoecology of the Tithonian–Berriasian brachiopods in the Pieniny Klippen Belt, Carpathians, Poland: Studia Geologica Polonica, v. 106, p. 89–156.

Krobicki, M., 1996, Neo-Cimmerian uplift of intraoceanic Czorsztyn pelagic swell (Pieniny Klippen Belt, Polish Carpathians) indicated by the changes of brachiopod assemblages: Georesearch Forum, v. 1–2, p. 255–264.

Ku, T.C., Walter, L.M., Coleman, M.L., Blake, R.E., and Martini, A.M., 1999, Coupling between sulfur recycling and syndepositional carbonate dissolution: Evidence from oxygen and sulfur isotope composition of pore-water sulfate, south Florida Platform, USA: Geochimica et Cosmochimica Acta, v. 63, p. 2529–2549.

Kulicki, C., and Wierzbowski, A., 1983, The Jurassic juvenile ammonites of the Jagua Formation, Cuba: Acta Palaeontologica Polonica, v. 28, p. 369–384.

Kutek, J., and Wierzbowski, A., 1979, Lower to Middle Tithonian ammonite succession at Rogoznik in the Pieniny Klippen Belt: Acta Geologica Polonica, v. 29, p. 195–205.

Landman, N.H., Rye, D.M., and Shelton, K.L., 1983, Early ontogeny of *Eutrephoceras* compared to Recent *Nautilus* and Mesozoic ammonites: Evidence from shell morphology and light stable isotopes: Paleobiology, v. 9, p. 269–279.

Landman, N.H., Tanabe, K., and Shigeta, Y., 1996, Ammonoid embryonic development, *in* Landman, N., et al., ed., Ammonoid Paleobiology: Topics in Geobiology: vol. 13, Plenum Press, New York, p. 343–405.

Laptikhovsky, V.V., and Nigmatulin, C.M., 1993, Egg size, fecundity, and spawning in females of the genus *Illex* (Cephalopoda: Ommastrephidae): ICES (International Council for the Exploration of the Sea) Journal of Marine Science, v. 50, p. 393–403.

Lescinsky, H.L., Edinger, E., and Risk, M.J., 2002, Mollusc shell encrustation and bioerosion rates in a modern epeiric sea: Taphonomy experiments in the Java Sea, Indonesia: PALAIOS, v. 17, p. 171–191.

Macintyre, I.G., 1977, Distribution of submarine cements in a modern Caribbean fringing reef, Galeta Point, Panama: Journal of Sedimentary Petrology, v. 47, p. 503–516.

Macintyre, I.G., 1984, Extensive submarine lithification in a cave in the Belize Barrier Reef Platform: Journal of Sedimentary Petrology, v. 54, p. 221–235.

Maeda, H., and Seilacher, A., 1996, Ammonoid taphonomy, *in* Landman, N., et al., ed., Ammonoid Paleobiology: Topics in Geobiology: vol. 13, Plenum Press, New York, p. 543–578.

Mamet, B., and Préat, A., 2006, Iron-bacterial mediation in Phanerozoic red limestones: State of the art: Sedimentary Geology, v. 185, p. 147–157.

Manger, W.L., Stephen, D.A., and Meeks, L.K., 1999, Possible cephalopod reproductive mass mortality reflected by Middle Carboniferous assemblages, Arkansas, southern United States, *in* Olóriz, F., and Rodríguez-Tovar, F.J., eds., Advancing Research on Living and Fossil Cephalopods: Kluwer Academic/Plenum Publishers, New York, p. 345–364.

Martin, R.E., 1996, Secular increase in nutrient levels through the phanerozoic: Implications for productivity, biomass, and diversity of the marine biosphere: PALAIOS, v. 11, p. 209–219.

Martire, L., 1992, Sequence stratigraphy and condensed pelagic sediments: An example from the Rosso Ammonitico Veronese: Palaeogeography, Palaeoclimatology, Palaeoecology, v. 94, p. 169–191.

Martire, L., 1996, Stratigraphy, facies and synsedimentary tectonics in the Jurassic Rosso Ammonitico Veronese (Altopiano di Asiago, NE Italy): Facies, v. 35, p. 209–236.

MARTIRE, L., and PAVIA, G., 1996, Taphonomic analysis of Bajocian ammonites from NW France (Normandy, Poitou): Georesearch Forum, v. 1–2, p. 305–316.
MCCLAIN, C.R., 2007, Seamounts: Identity crisis or split personality: Journal of Biogeography, v. 34, p. 2001–2008.
MILLER, A.I., and CUMMINS, H., 1990, A numerical model for the formation of fossil assemblages: Estimating the amount of post-mortem transport along environmental gradients: PALAIOS, v. 5, p. 303–316.
MILLIMAN, J.D., ROSS, D.A., and KU, T.-L., 1969, Precipitation of deep-sea carbonates in the Red Sea: Journal of Sedimentary Petrology, v. 39, p. 724–736.
MIŠÍK, M., and SÝKORA, M., 1993, Jurassic submarine scarp breccia and neptunian dykes from the Kyjov–Pusté Pole klippen (Czorsztyn Unit): Mineralia Slovaca, v. 25, p. 411–427.
MOLTSCHANIWSKYJ, N.A., and STEER, M.A., 2004, Spatial and seasonal variation in reproductive characteristics and spawning of southern calamary (*Sepioteuthis australis*): Spreading the mortality risk: ICES (International Council for the Exploration of the Sea) Journal of Marine Science, v. 61, p. 921–927.
MUNNECKE, A., and WESTPHAL, H., 2005, Variations in primary aragonite, calcite, and clay in fine-grained calcareous rhythmites of Cambrian to Jurassic age—An environmental archive?: Facies, v. 51, p. 592–607.
NEUWEILER, F., and BERNOULLI, D., 2005, Mesozoic (Lower Jurassic) red stromatactis limestones from the southern Alps (Arzo, Switzerland): Calcite mineral authigenesis and syneresis-type deformation: International Journal of Earth Sciences, v. 94, p. 130–146.
OKSANEN, J., KINDT, R., and OHARA, B., 2005, The Vegan Package: R language, http://cc.oulu.fi/~jarioksa/softhelp/vegan.html. Checked June 2008.
OLÓRIZ, F., CARACUEL, J.E., RUIZ-HERAS, J.J., RORDÍGUEZ-TOVAR, F.J., and MARQUES, B., 1996, Ecostratigraphic approaches, sequence stratigraphy proposals and block tectonics: Examples from epioceanic swell areas in south and east Iberia: Palaeogeography, Palaeoclimatology, Palaeoecology, v. 121, p. 273–295.
OLÓRIZ, F., REOLID, M., and RODRÍGUEZ-TOVAR, F.J., 2002, Fossil assemblages, lithofacies, taphofacies and interpreting depositional dynamics in the epicontinental Oxfordian of the Prebetic Zone, Betic Cordillera, southern Spain: Palaeogeography, Palaeoclimatology, Palaeoecology, v. 185, p. 53–75.
OLÓRIZ, F., REOLID, M., and RODRÍGUEZ-TOVAR, F.J., 2004, Microboring and taphonomy in Middle Oxfordian to lowermost Kimmeridgian (Upper Jurassic) from the Prebetic Zone (southern Iberia): Palaeogeography, Palaeoclimatology, Palaeoecology, v. 212, p. 181–197.
OLÓRIZ, F., VILLASEÑOR, A.B., and GONZÁLEZ-ARREOLA, C., 1997, Factors controlling upper Jurassic ammonite assemblages in north-central Mexico: Lethaia, v. 30, p. 337–351.
OLSZEWSKI, T., 1999, Taking advantage of time-averaging: Paleobiology, v. 25, p. 226–238.
OLSZEWSKI, T., 2004, Modeling the influence of taphonomic destruction, reworking, and burial on time-averaging in fossil accumulations: PALAIOS, v. 19, p. 39–50.
PALMER, T.J., and WILSON, M.A., 2004, Calcite precipitation and dissolution of biogenic aragonite in shallow Ordovician calcite seas: Lethaia, v. 37, p. 417–427.
PAYNE, J.L., and FINNEGAN, S., 2006, Controls on marine animal biomass through geological time: Geobiology, v. 4, p. 1–10.
PAYNE, J.L., LEHRMANN, D.L., WEI, J., and KNOLL, A.H., 2006, The Pattern and Timing of Biotic Recovery from the End-Permian Extinction on the Great Bank of Guizhou, Guizhou Province, China: PALAIOS, v. 21, p. 63–85.
PECL, G.T., 2004, The in situ relationships between season of hatching, growth and condition in the southern calamary, *Sepioteuthis australis*: Marine and Freshwater Research, v. 55, p. 429–438.
PERRY, C.T., and TAYLOR, K.G., 2006, Inhibition of dissolution within shallow water carbonate sediments: Impacts of terrigenous sediment input on syn-depositional carbonate diagenesis: Sedimentology, v. 53, p. 495–513.
PETERS, S.E., 2004, Evenness of Cambrian–Ordovician benthic marine communities in North America: Paleobiology, v. 30, p. 325–346.
POWELL, E.N., 1992, A model for death assemblage: Can sediment shelliness be explained?: Journal of Marine Research, v. 50, p. 229–265.
POWELL, E.N., CALLENDER, W.R., STAFF, G.M., PARSONS-HUBBARD, K.M., BRETT, C.E., WALKER, S.E., RAYMOND, A., and ASHTON-ALCOX, K.A., 2008, Molluscan shell condition after eight years on the sea floor—Taphonomy in the Gulf of Mexico and Bahamas: Journal of Shellfish Research, v. 27, p. 191–225.
PRÉAT, A., MORANO, S., LOREAU, J.L., DURLET, C., and MAMET, B., 2006, Petrography and biosedimentology of the Rosso Ammonitico Veronese (middle–upper Jurassic, north-eastern Italy): Facies, v. 52, p. 265–278.
PRETO, N., SPÖTL, C., MIETTO, P., GIANOLLA, P., RIVA, A., and MANFRIN, S., 2005, Aragonite dissolution, sedimentation rates and carbon isotopes in deep-water hemipelagites (Livinallongo Formation, Middle Triassic, northern Italy): Sedimentary Geology, v. 181, p. 173–194.
QUINN, G.P., and KEOUGH, M.J., 2002, Experimental design and data analysis for biologists: Cambridge University Press, Cambridge, UK.
REBOULET, S., MATTIOLI, E., PITTET, B., BAUDIN, F., OLIVERO, D., and PROUX, O., 2003, Ammonoid and nannoplankton abundance in Valanginian (early Cretaceous) limestone-marl successions from the southeast France Basin: Carbonate dilution or productivity?: Palaeogeography, Palaeoclimatology, Palaeoecology, v. 201, p. 113–139.
REHÁKOVÁ, D., 2000, Calcareous dinoflagellate and calpionellid bioevents versus sea-level fluctuations recorded in the West-Carpathian (Late Jurassic/Early Cretaceous) pelagic environments: Geologica Carpathica, v. 51, p. 229–243.
RIDING, R., and LIANG, L., 2005, Geobiology of microbial carbonates: Metazoan and seawater saturation state influences on secular trends during the Phanerozoic: Palaeogeography, Palaeoclimatology, Palaeoecology, v. 219, p. 101–115.
SANDBERG, P.A., 2003, An oscillating trend in Phanerozoic nonskeletal carbonate mineralogy: Nature, v. 305, p. 19–22.
SANDERS, D., 2001, Burrow-mediated carbonate dissolution in rudist biostromes (Aurisina, Italy): Implications for taphonomy in tropical, shallow subtidal carbonate environments: Palaeogeography, Palaeoclimatology, Palaeoecology, v. 168, p. 39–74.
SANDERS, D., 2003, Syndepositional dissolution of calcium carbonate in neritic carbonate environments: Geological recognition, processes, potential significance: Journal of African Earth Sciences, v. 36, p. 99–134.
SANTANTONIO, M., 1993, Facies associations and evolution of pelagic carbonate platform/basin systems: Examples from the Italian Jurassic: Sedimentology, v. 40, p. 1039–1067.
SANTANTONIO, M., 1994, Pelagic carbonate platforms in the geologic record: Their classification, and sedimentary and paleotectonic evolution: American Association of Petroleum Geology Bulletin, v. 78, p. 122–141.
SEBENS, K.P., 1987, The ecology of indeterminate growth in animals: Annual Reviews of Ecology and Systematics, v. 18, p. 371–407.
SHIGETA, Y., 1993, Post-hatching early life history of Cretaceous Ammonoidea: Lethaia, v. 26, p. 133–145.
STEER, M.A., MOLTSCHANIWSKYJ, N.A., and GOWLAND, F.C., 2002, Temporal variability in embryonic development and mortality in the southern calamary *Sepioteuthis australis*: A field assessment: Marine Ecology Progress Series, v. 243, p. 143–150.
STILLMAN, R.A., MCGROTRY, S., GOSS-CUSTARD, J.D., and WEST, A.D., 2000, Predicting mussel population density and age structure: The relationship between model complexity and predictive power: Marine Ecology Progress Series, v. 208, p. 131–145.
TANABE, K., LANDMAN, H., MAPES, R.H., and FAULKNER C.J., 1993, Analysis of a Carboniferous embryonic ammonoid assemblage from Kansas U.S.A. Implications for ammonoid embryology: Lethaia, v. 26, p. 215–224.
TANABE K., SHIGETA Y., and MAPES, R.H., 1995, Early life history of Carboniferous ammonoids inferred from analysis of fossil assemblages and shell hydrostatics: PALAIOS, v. 10, p. 80–86.
TOMAŠOVÝCH, A., 2006, Linking taphonomy to community-level abundance: Insights into compositional fidelity of the Upper Triassic shell concentrations (Eastern Alps): Palaeogeography, Palaeoclimatology, Palaeoecology, v. 235, p. 355–381.
TOMAŠOVÝCH, A., FÜRSICH, F.T., and OLSZEWSKI, T.D., 2006, Modeling shelliness and alteration in shell beds: Variation in hardpart-input and burial rates leads to opposing predictions: Paleobiology, v. 32, p. 278–298.
TUCKER M.E., and WRIGHT, V.P. 1990, Carbonate Sedimentology: Blackwell, Oxford, UK, 482 p.
VAN DER KOOIJ, B., IMMENHAUSER, A., STEUBER, T., HAGMAIER, M., BAHAMONDE, J.R., SAMANKASSOU, E., and MERINO TOMÉ, O., 2007, Marine red staining of a Pennsylvanian carbonate slope: Environmental and oceanographic significance: Journal of Sedimentary Research, v. 77, p. 1026–1045.
VAN DER MEER, J., BEUKEMA, J.J., and DEKKER, R., 2001, Long-term variability in secondary production of an intertidal bivalve population is primarily a matter of recruitment variability: Journal of Animal Ecology, v. 70, p. 159–169.
WALTER, L.M., BISCHOF, S.A., PATTERSON, W.P., and LYONS, T.W., 1993, Dissolution and Recrystallization in Modern Shelf Carbonates: Evidence from Pore Water and Solid Phase Chemistry: Philosophical Transactions: Physical Sciences and Engineering, v. 344, p. 27–36.
WALTER, L.M., and BURTON, E.A., 1990, Dissolution of Recent platform carbonate sediments in marine pore fluids: American Journal of Science, v. 290, p. 601–643.
WALUDA, C.M., RODHOUSE, P.G., PODESTÁ, G.P., TRATHAN, P.N., and PIERCE, G.J., 2001, Surface oceanography of the inferred hatching grounds of *Illex argentinus* (Cephalopoda: Ommastrephidae) and influences on recruitment variability: Marine Biology, v. 139, p. 671–679.
WALUDA, C.M., TRATHAN, P.N., and RODHOUSE, P.G., 1999, Influence of oceanographic variability on recruitment in the *Illex argentinus* (Cephalopoda: Ommastrephidae) fishery in the South Atlantic: Marine Ecology Progress Series, v. 183, p. 159–167.
WARD, P.D., and BANDEL, K., 1987, Life history strategies in fossil cephalopods, *in* Boyle P.R., ed., Cephalopod Life Cycles: vol. 2, Academic Press, London, p. 329–350.

WATKINSON, A.R., 1980, Density-dependence in single-species populations of plants: Journal of Theoretical Biology, v. 83, p. 345–357.

WATKINSON, A.R., GILL, J.A., and FRECKLETON, R.P., 2003, Macroecology and microecology: Linking large-scale patterns of abundance to population processes, *in* Blackburn, T.M., and Gaston, K.J., eds., Macroecology: Concepts and Consequences: Blackwell, Oxford, UK, p. 256–273.

WELLS, M.J., and CLARKE, A., 1996, Energetics: The costs of living and reproducing for an individual cephalopod: Philosophical Transactions of the Royal Society London, ser. B, v. 351, p. 1083–1104.

WENDT, J., 1973, Cephalopod accumulations in the Middle Triassic Hallstatt-Limestone of Jugoslavia and Greece: Neues Jahrbuch für Geologie und Paläontologie, Monatshefte, v. 1973, p. 189–206.

WENDT, J., AIGNER, T., and NEUGEBAUER, J., 1984, Cephalopod limestone deposition on a shallow pelagic ridge: The Tafilalt Platform: Sedimentology, v. 31, p. 601–625.

WESTPHAL, H., 2006, Limestone-marl alternations as environmental archives and the role of early diagenesis: A critical review: International Journal of Earth Sciences, v. 95, p. 947–961.

WESTPHAL, H., HEAD, M.J., and MUNNECKE, A., 2000, Differential diagenesis of rhythmic limestone alternations supported by palynological evidence: Journal of Sedimentary Research, v. 70, p. 715–725.

WHEELEY, J.R., CHERNS, L., and WRIGHT, P., 2008, Provenance of microcrystalline carbonate cement in limestone-marl alternations (LMA): Aragonite mud or molluscs?: Journal of the Geological Society, v. 165, p. 395–403.

WIGNALL, P.B., and BENTON, M.J., 1999, Lazarus taxa and fossil abundance in times of biotic crisis: Journal of the Geological Society, v. 156, p. 453–456.

WILSON, P.A., and DICKSON, J.A.D., 1996, Radiaxial calcite: Alteration product of and petrographic proxy for magnesian calcite marine cement: Geology, v. 24, p. 945–948.

WRIGHT, P., CHERNS, L., and HODGES, P., 2003, Missing molluscs: Field testing taphonomic loss in the Mesozoic through early large-scale aragonite dissolution: Geology, v. 31, p. 211–214.

ZEMPOLICH, W.G., 1993, The drowning succession in Jurassic carbonates of the Venetian Alps, Italy: A record of supercontinental breakup, gradual eustatic rise, and eutrophication of shallow-water environments: AAPG (American Association of Petroleum Geologists) Memoirs, v. 57, p. 63–105.

ZUSCHIN, M., HARZHAUSER, M., and MANDIC, O., 2005, Influence of size-sorting on diversity estimates from tempestitic shell beds in the middle Miocene of Austria: PALAIOS, v. 20, p. 142–158.

ACCEPTED MAY 12, 2008